Magnetic hybrid sol-gel ionic network catalyst for direct alcohol esterification under solvent-free conditions

Maryam Faraji,[a] Fariborz Mansouri,* [b] Babak Karimi*[a,c] and Hojatollah Vali[d]

[a]Department of Chemistry, Institute for Advanced Studies in Basic Sciences (IASBS), Prof. Sobouti Boulevard, Zanjan 45137-66731, Iran.

[b]Department of Chemical Technologies, Iranian Research Organization for Science and Technology (IROST), Tehran, Iran

[C]Research Centre for Basic Sciences & Modern Technologies (RBST), Institute for Advanced Studies in Basic Sciences (IASBS), Zanjan 45137-66731, Iran

[d] Department of Anatomy, Cell Biology and Facility for Electron Microscopy Research, McGill University, Montreal, Quebec H3A 2A7, Canada

Table of content

Tables

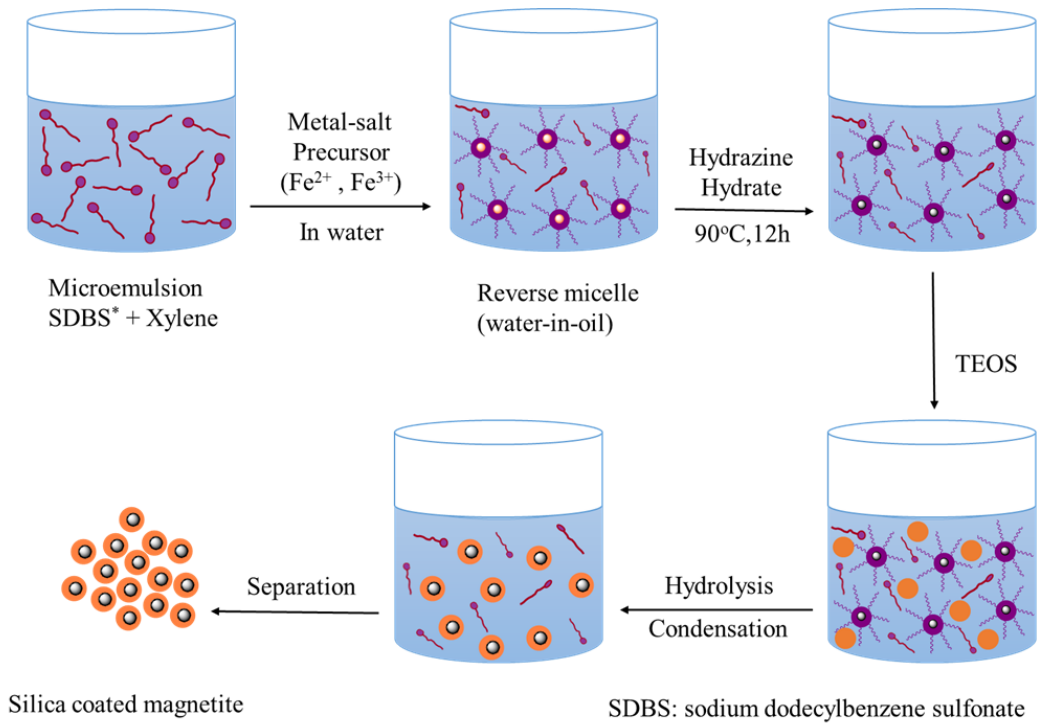

Figure S1: Microemulsion method to prepare Fe_3O_4@SiO_2 core-shell nanoparticles

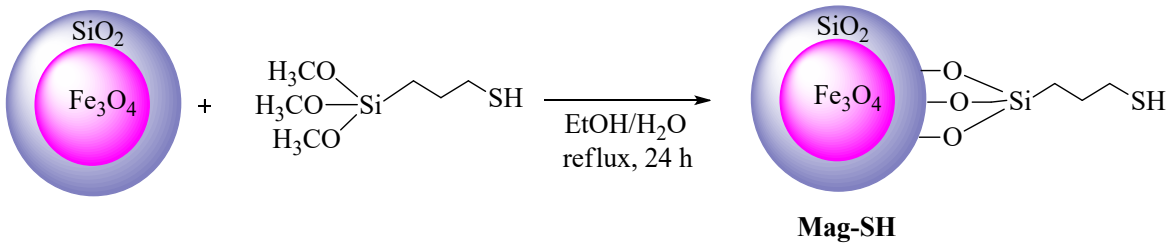

Figure S2: Stabilization of 3-mercaptopropyltrimethoxysilane on Fe_3O_4@SiO_2

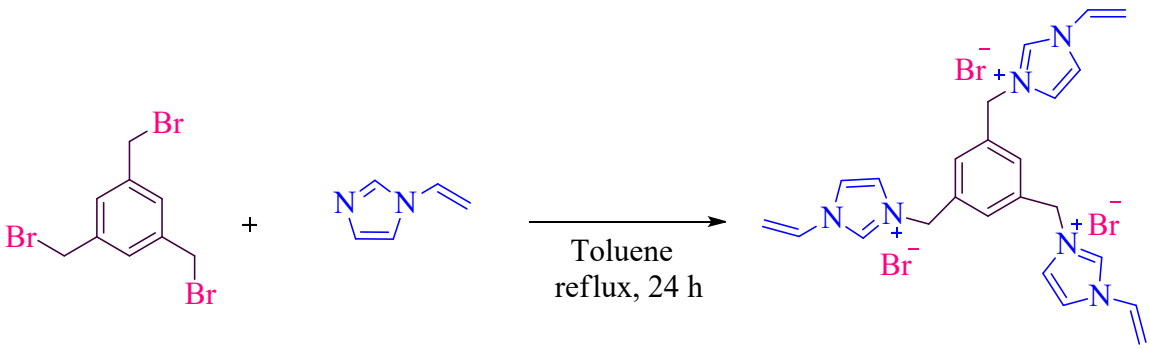

Figure S3:Preparation method of 1,3,5-tris (vinylimidazolemethyl)benzene bromide

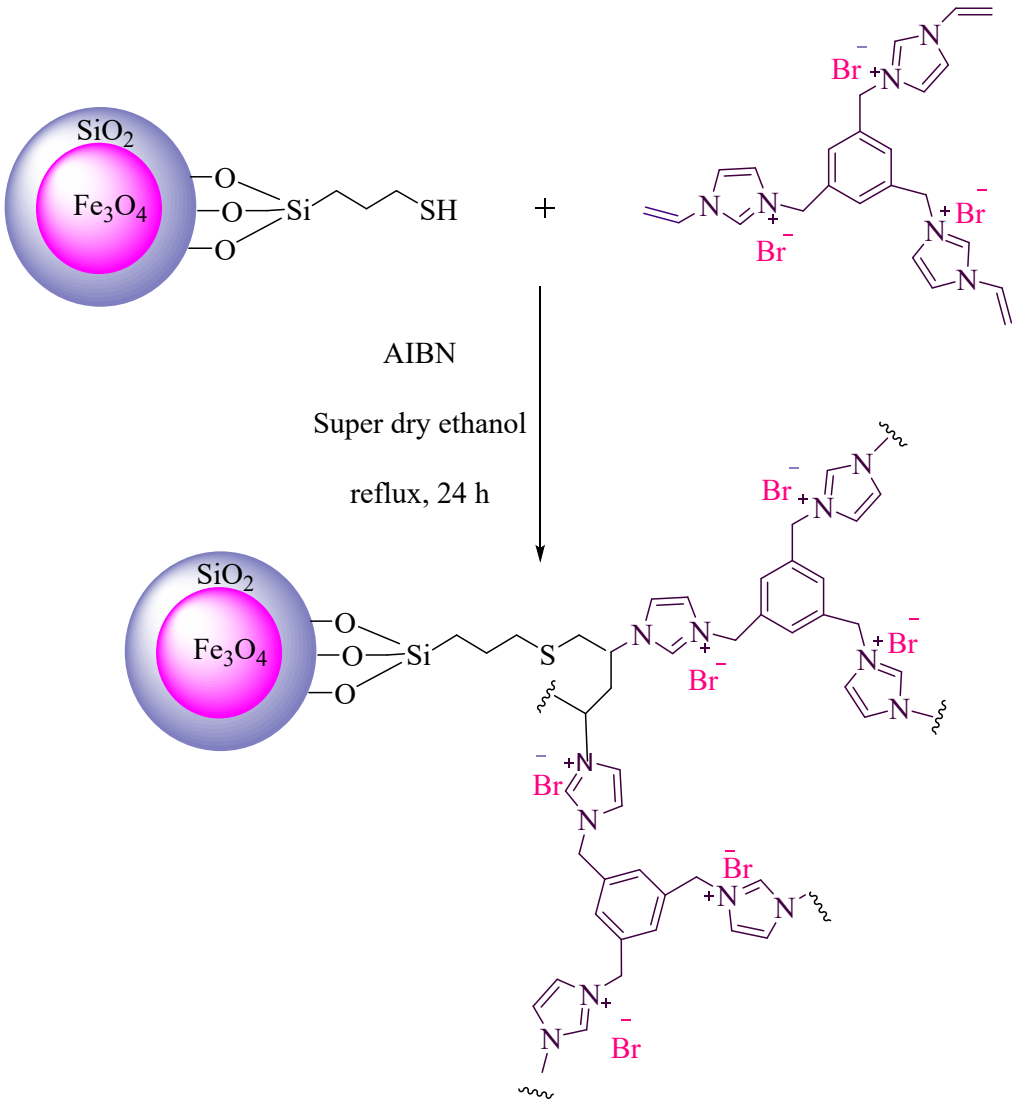

Fe_3O_4@SiO_2-S-xIm$^+$Br$^-$

Figure S4: Immobilization of ionic liquid on Fe_3O_4@SiO_2-SH

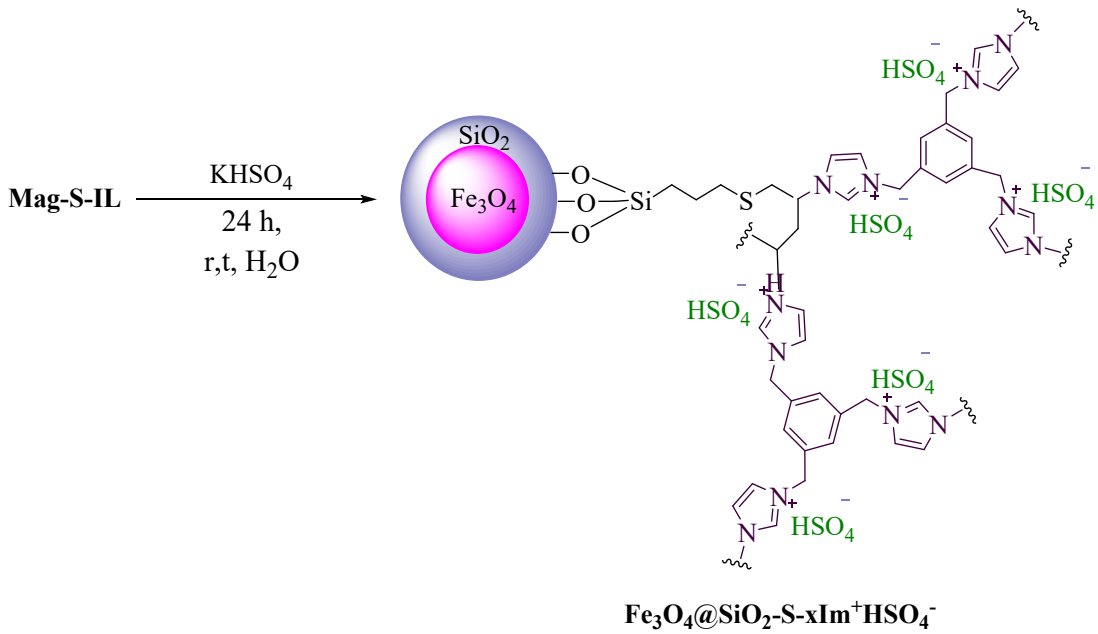

Figure S5: The method of exchanging hydrogen sulfate anion with bromide ion on Fe_3O_4@SiO_2-S-xIm$^+$Br$^-$ magnetic support

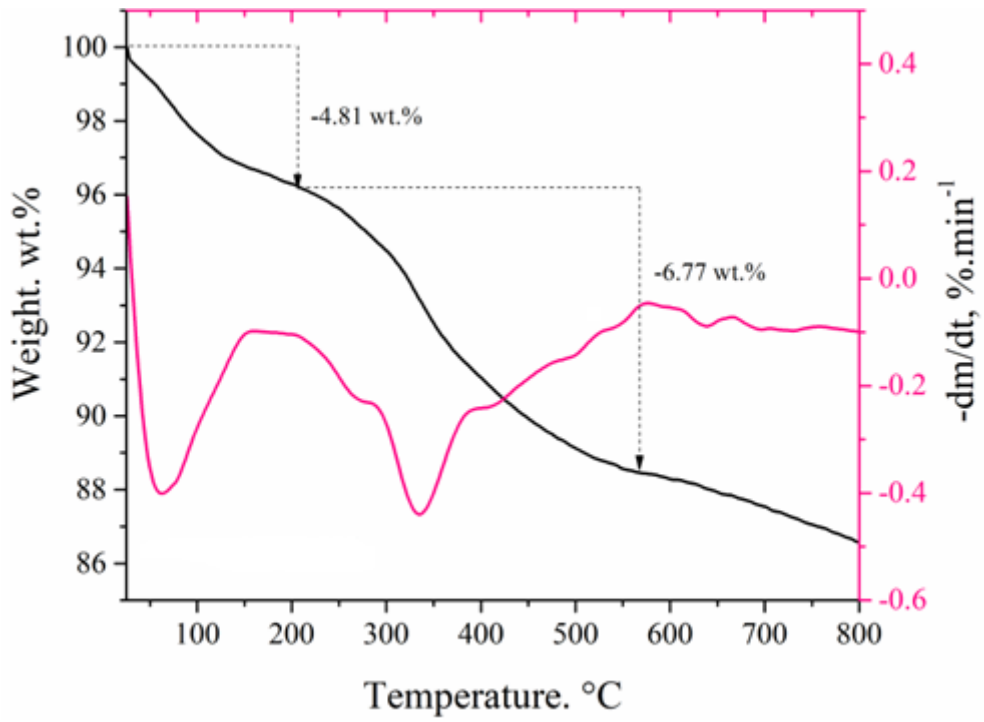

Figure S6: TG analysis of Fe_3O_4@SiO_2-SH

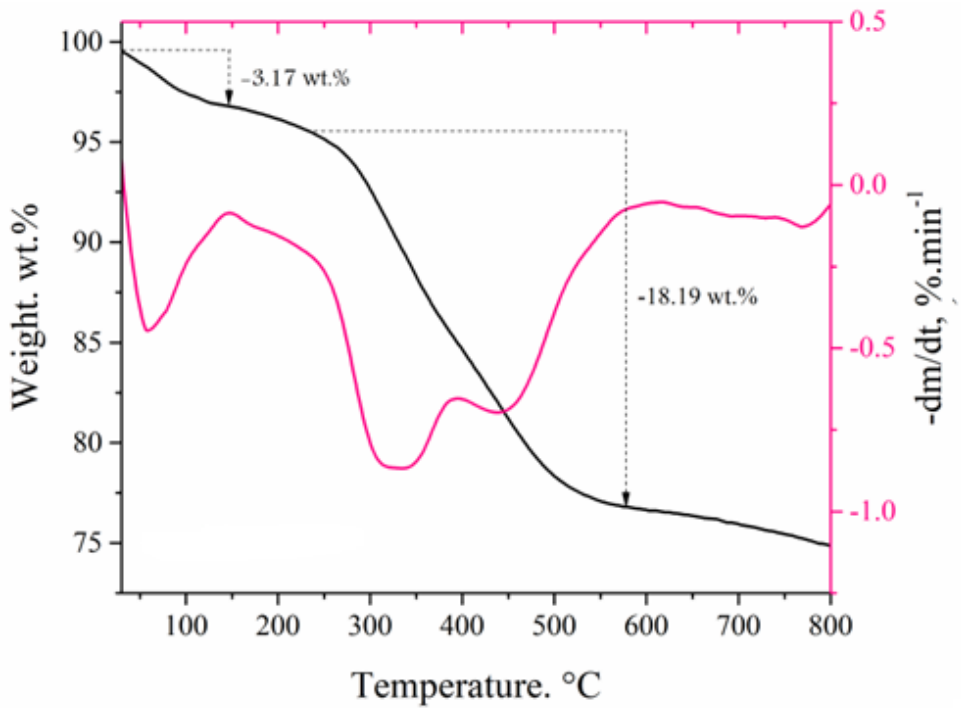

Figure S7: TG analysis of Fe_3O_4@SiO_2-S-xIm$^+$Br$^-$

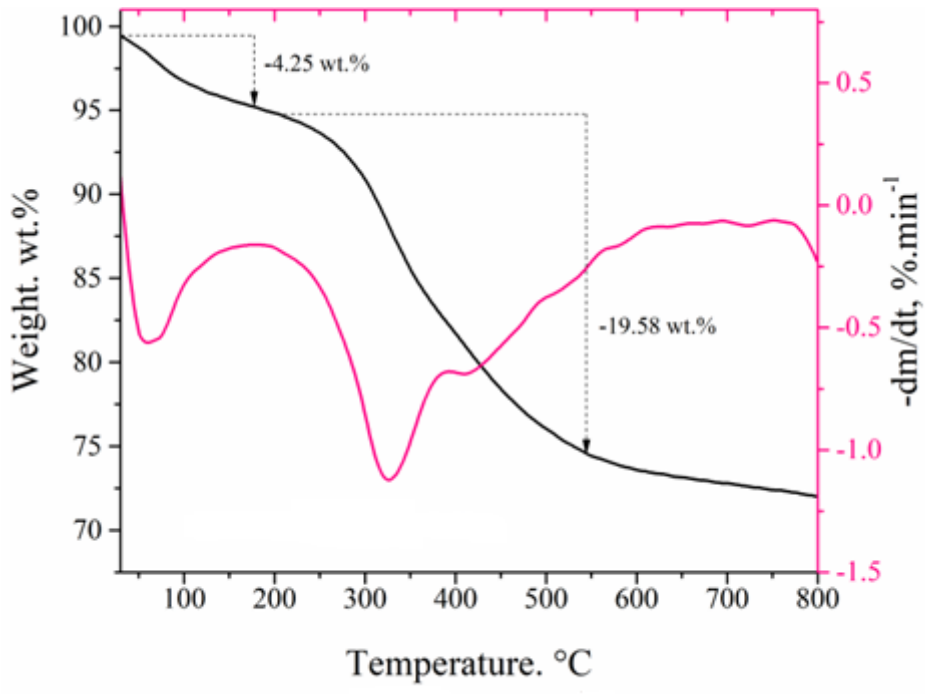

Figure S8 :TG analysis of Fe_3O_4@SiO_2-S-xIm$^+$HSO$_4^-$

Table S1 :CHNS analysis of prepared material

Sample	S (%)	H (%)	N (%)	C (%)	Loading of organic

					species
$Fe_3O_4@SiO_2$-SH	2.06	0.5	--	2.66	0.64 mmol/gr [a]
$Fe_3O_4@SiO_2$-S-xIm^+Br^-	2.122	0.849	2.103	9.63	0.75 mmol/ gr [b]
$Fe_3O_4@SiO_2$-S-x$Im^+HSO_4^-$	3.761	1.126	2.037	10.66	0.51 mmol/gr [c]

[a] based on sulfur percentage of mercaptopropyltrimethoxysilane

[b] based on nitrogen percentage of ionic liquid

[c] based on sulfur percentage of hydrogen sulfate

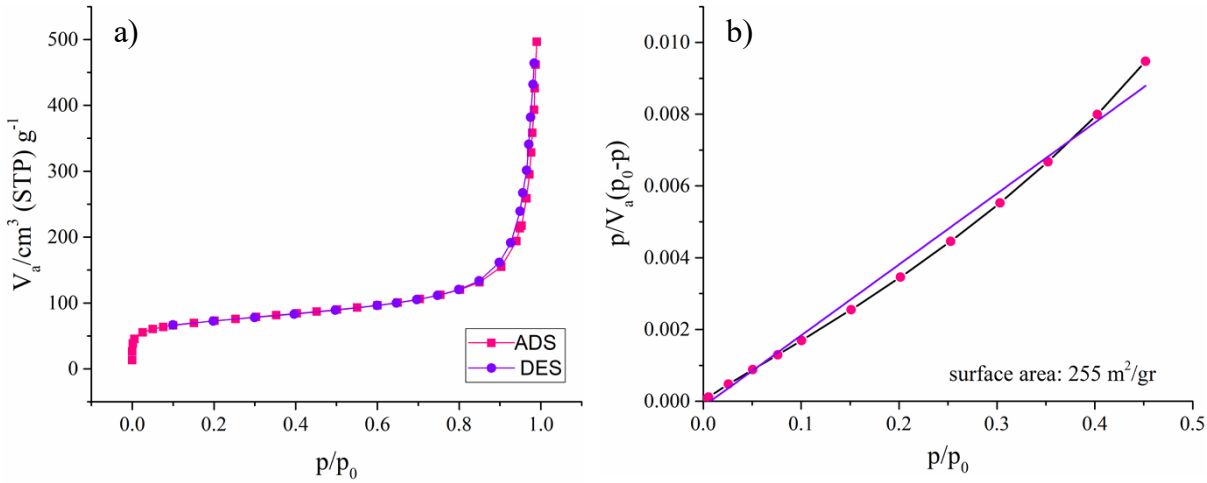

Figure S9 :Nitrogen adsorption-desorption (a, BET isotherm of $Fe_3O_4@SiO_2$

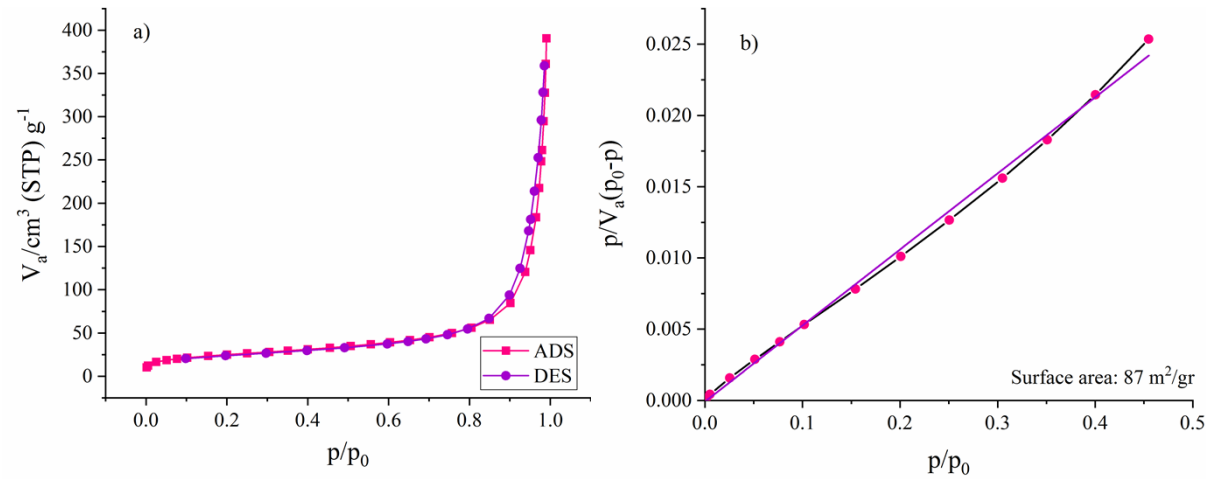

Figure S10 :Nitrogen adsorption-desorption (a, BET isotherm of $Fe_3O_4@SiO_2$-SH

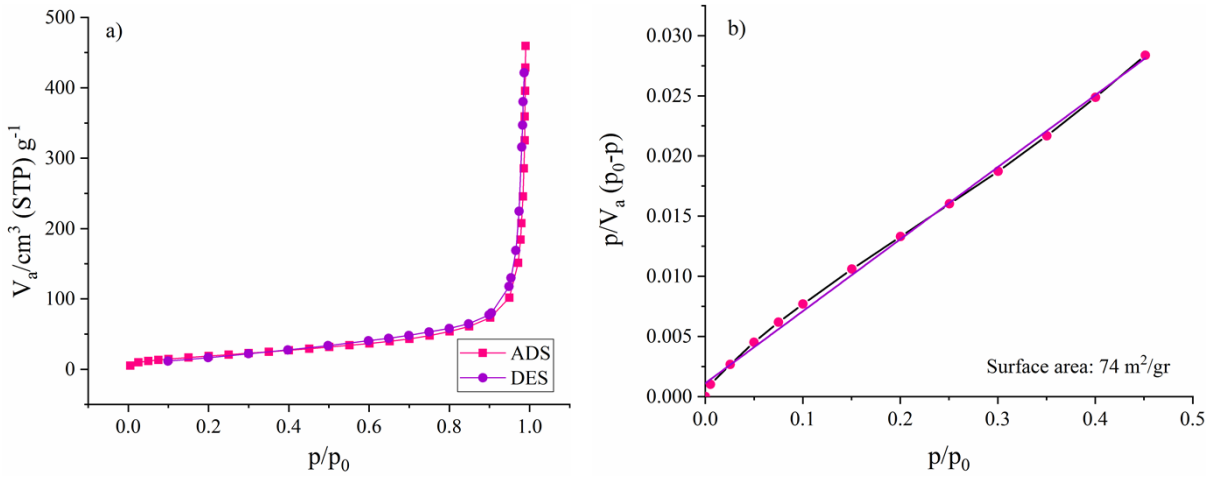

Figure S11:Nitrogen adsorption-desorption (a, BET isotherm of Fe_3O_4@SiO_2-S-xIm$^+$Br$^-$

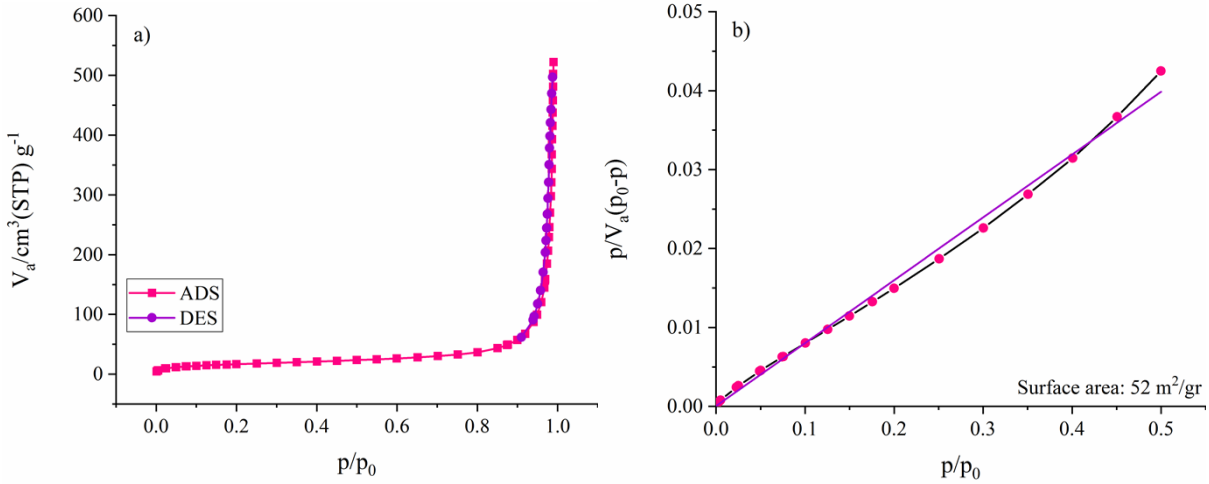

Figure S12 :Nitrogen adsorption-desorption (a, BET isotherm of Fe_3O_4@SiO_2-S-xIm$^+$HSO$_4^-$

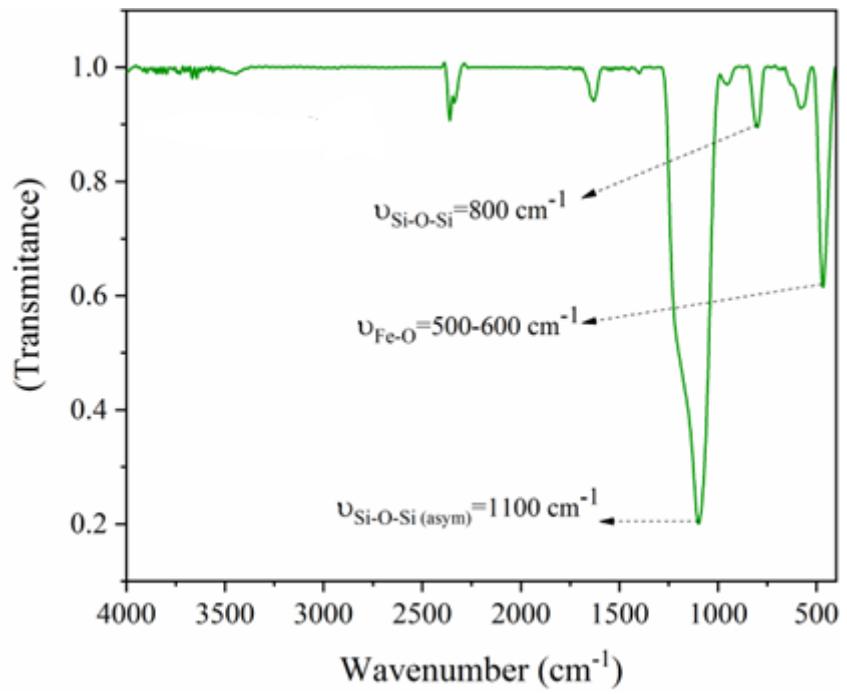

Figure S13 :FT-IR spectra for Fe_3O_4@SiO_2 core-shell nanoparticle

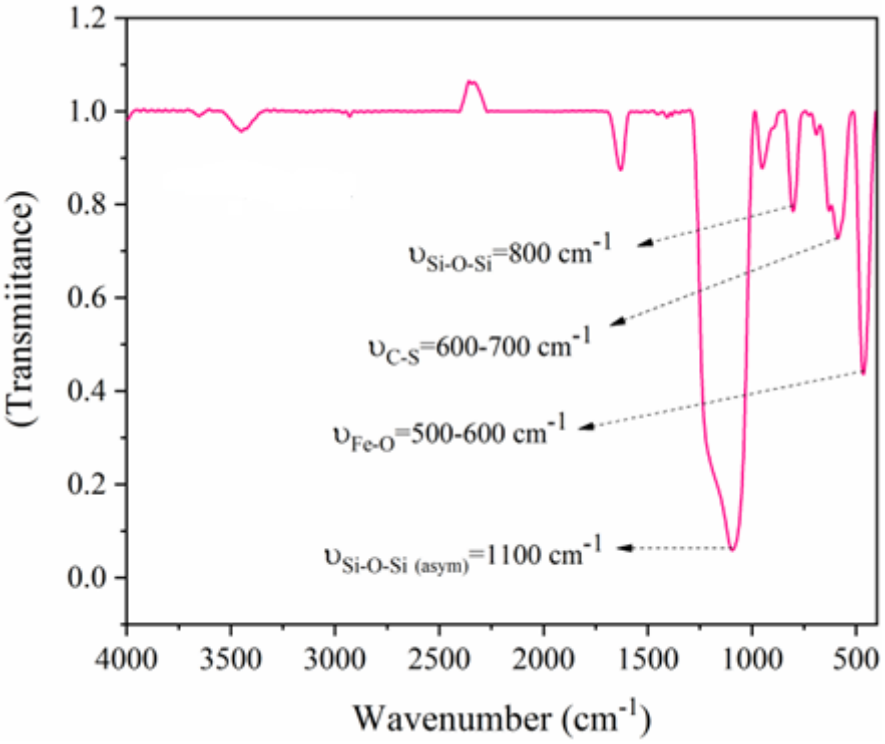

Figure S14 :FT-IR spectra for Fe_3O_4@SiO_2-SH

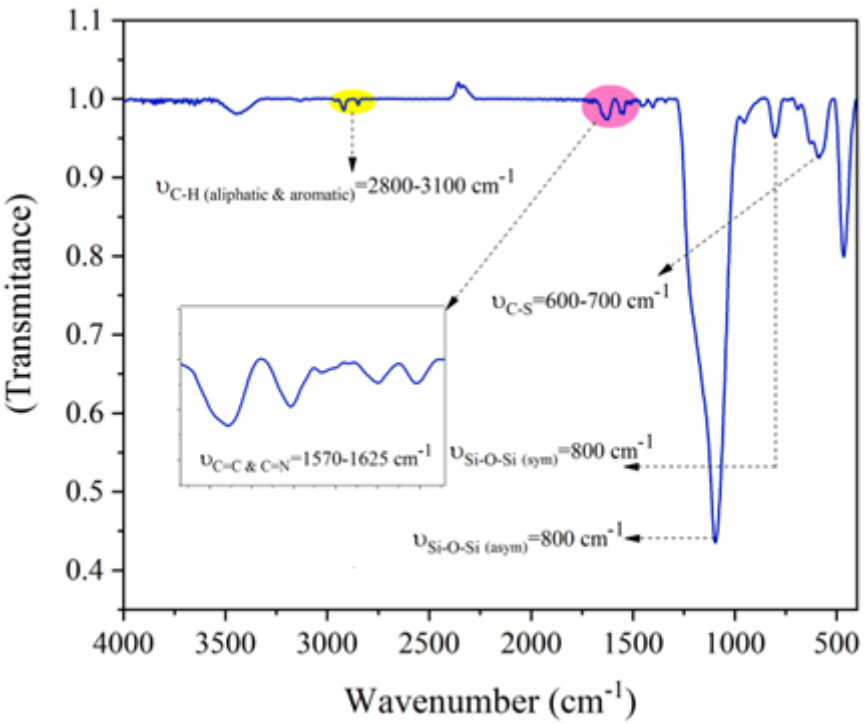

Figure S15 :FT-IR spectra for Fe_3O_4@SiO_2-S-xIm$^+$Br$^-$

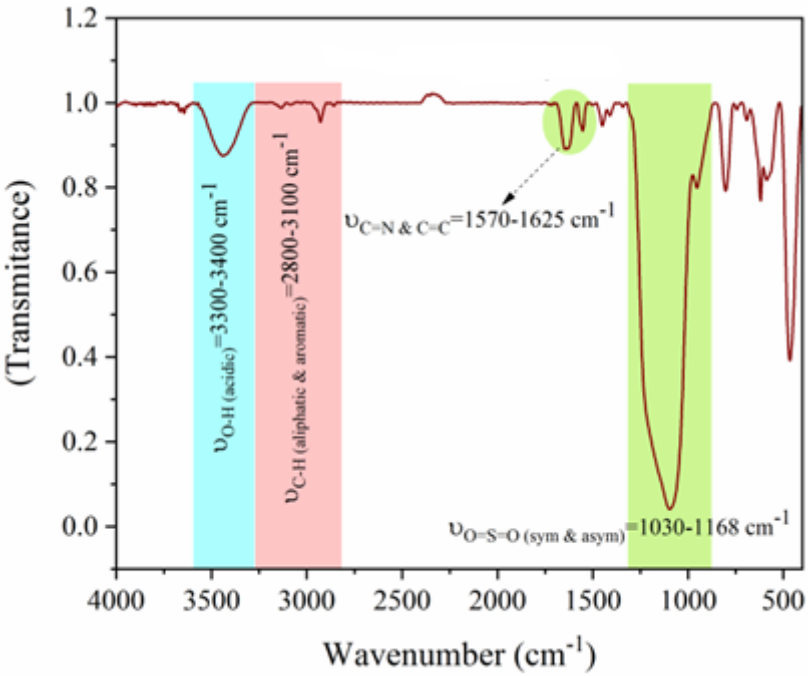

Figure S16 :FT-IR spectra for Fe_3O_4@SiO_2-S-xIm$^+$HSO$_4^-$

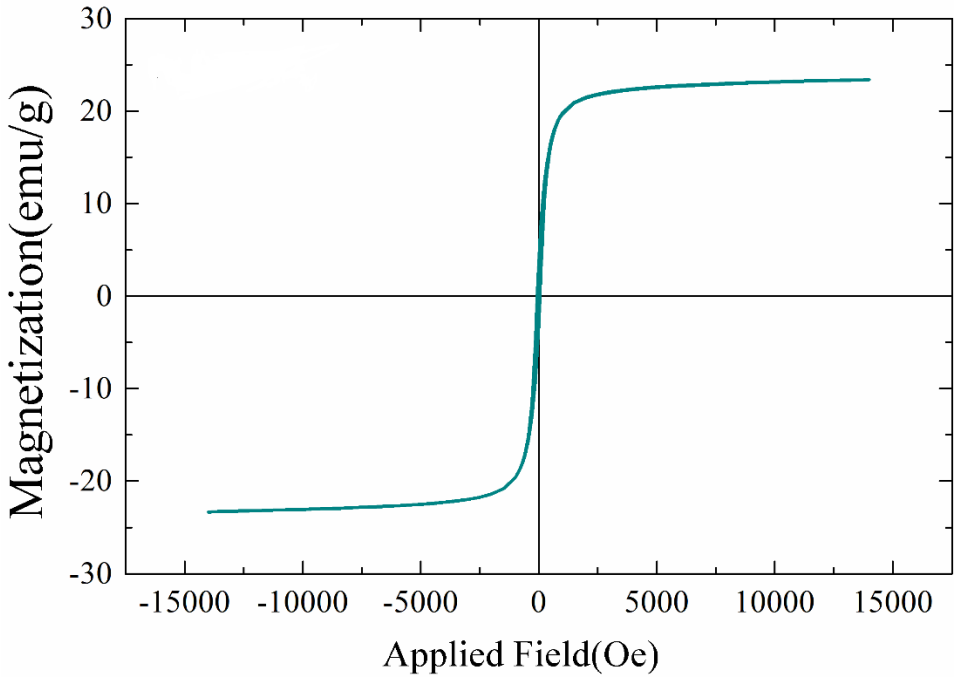

Figure S17 :The VSM curves of Fe_3O_4@SiO_2

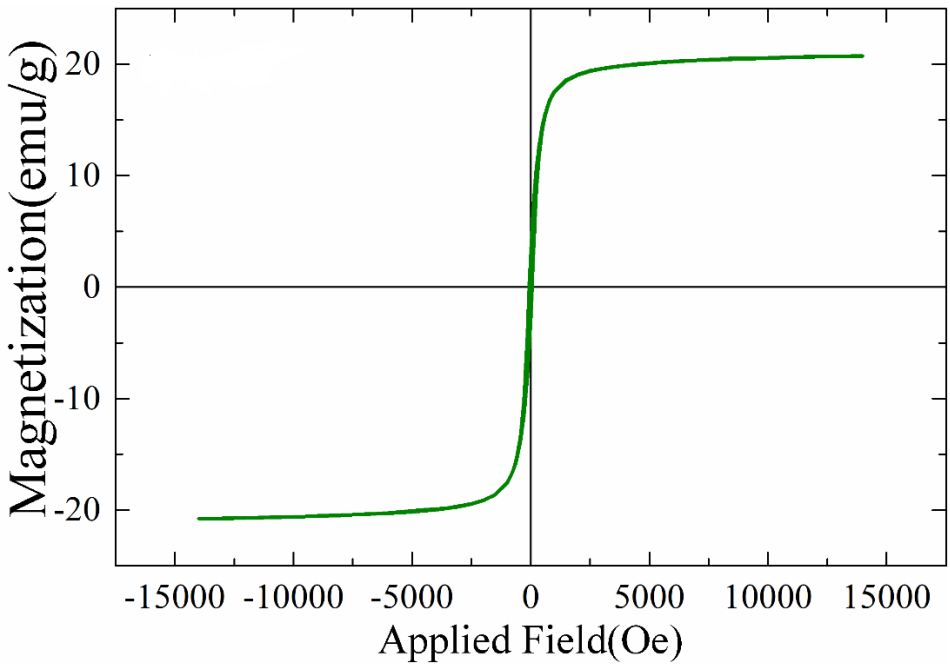

Figure S18 :The VSM curves of Fe_3O_4@SiO_2-SH

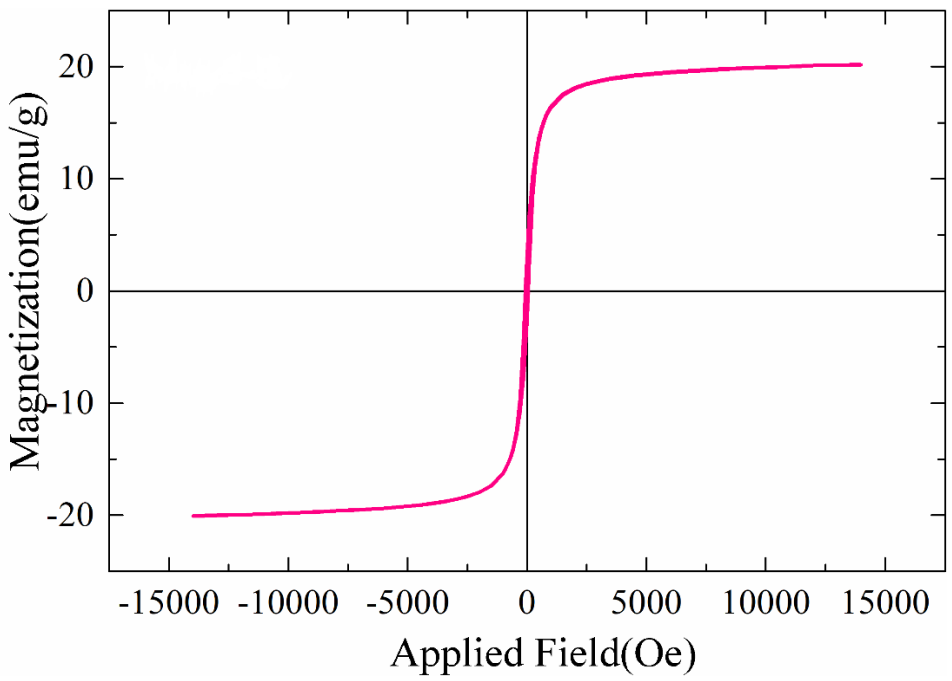

Figure S19 :The VSM curves of Fe_3O_4@SiO_2-S-xIm^+Br^-

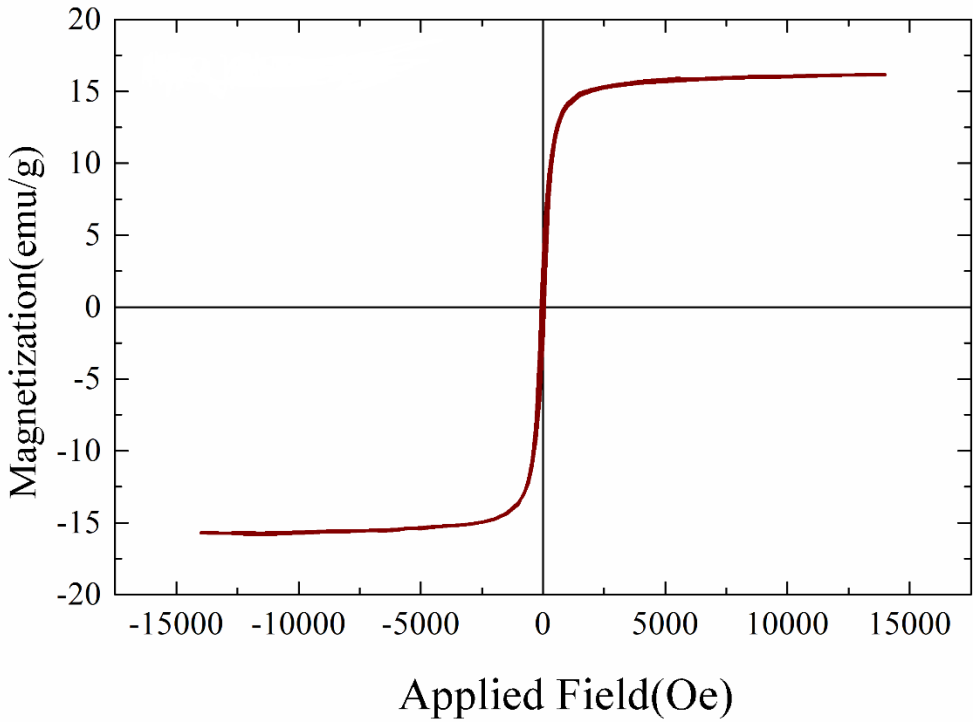

Figure S20 :The VSM curves of Fe_3O_4@SiO_2-S-x$Im^+HSO_4^-$

Table S2 :investigation of catalytic performance of $Fe_3O_4@SiO_2$-S-XIm$^+HSO_4^-$ in primary alcohols

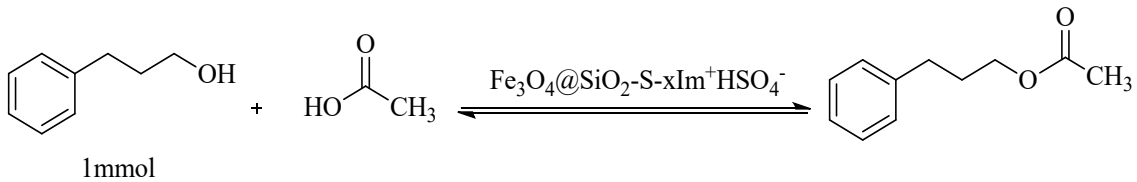

Entry	Catalyst (mol%)	Temp (°C)	Time (h)	Acetic acid (mmol)	Yield (%)
1	5	45	10	2.5	15
2	5	45	20	2.5	29
3	5	45	40	2.5	76
4	1	45	40	2.5	27
5	1	65	40	2.5	76
6	1	75	40	2.5	98
7	0.5	75	40	2.5	79
8	0.5	85	40	2.5	100
9	0.5	85	5	2.5	53
10	0.5	85	10	2.5	55
11	0.5	85	15	2.5	75
12	0.5	85	20	2.5	83
13	0.5	85	25	2.5	98
14	0.5	85	30	2.5	100
15	0.2	85	1	2.5	12
16	0.2	85	2	2.5	16
17	0.2	85	3	2.5	26
18	0.2	85	4	2.5	32
19	0.2	85	5	2.5	35
20	0.2	85	8	2.5	44
21	0.2	85	10	2.5	66
22	0.2	85	12	2.5	74
23	0.2	85	15	2.5	79
24	0.2	85	20	2.5	82
25	0.2	85	23	2.5	86
26	0.2	85	25	2.5	87
27	0.2	85	30	2.5	89
28	0.2	85	35	2.5	94

29	0.2	85	40	2.5	100
30	0.5	85	40	1.5	63
31	0.2	85	40	1.5	65
32	0.5	85	10	5	86
33	0.5	85	15	5	100
34	0.5	85	20	5	100
35	0.5	85	25	5	100
36	0.2	85	10	5	94
37	0.2	85	15	5	100
38	0.2	85	20	5	100
39	0.2	85	25	5	100
40	**0.1**	85	**15**	5	**98**
41	0.1	85	24	5	100

Table S3: investigation of catalytic performance of Fe_3O_4@SiO_2-S-XIm$^+$HSO$_4^-$ in secondary alcohols

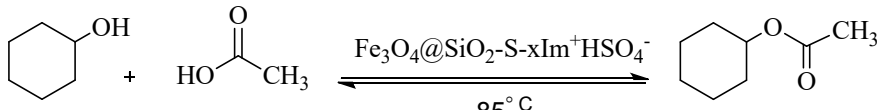

1mmol

Entry	Catalyst (mol%)	Time (h)	Acetic acid (mmol)	Yield (%)
1	0.1	15	5	55
2	0.2	15	5	57
3	0.2	24	5	63
4	0.3	15	5	52
5	0.3	20	5	60
6	0.3	24	5	61
7	0.2	15	7	63
8	0.2	20	7	68
9	0.2	24	7	73
10	0.1	15	7	69
11	**0.1**	**24**	**7**	**90**
12	0.1	15	10	75
13	0.1	24	10	90

14	0.1	30	10	93

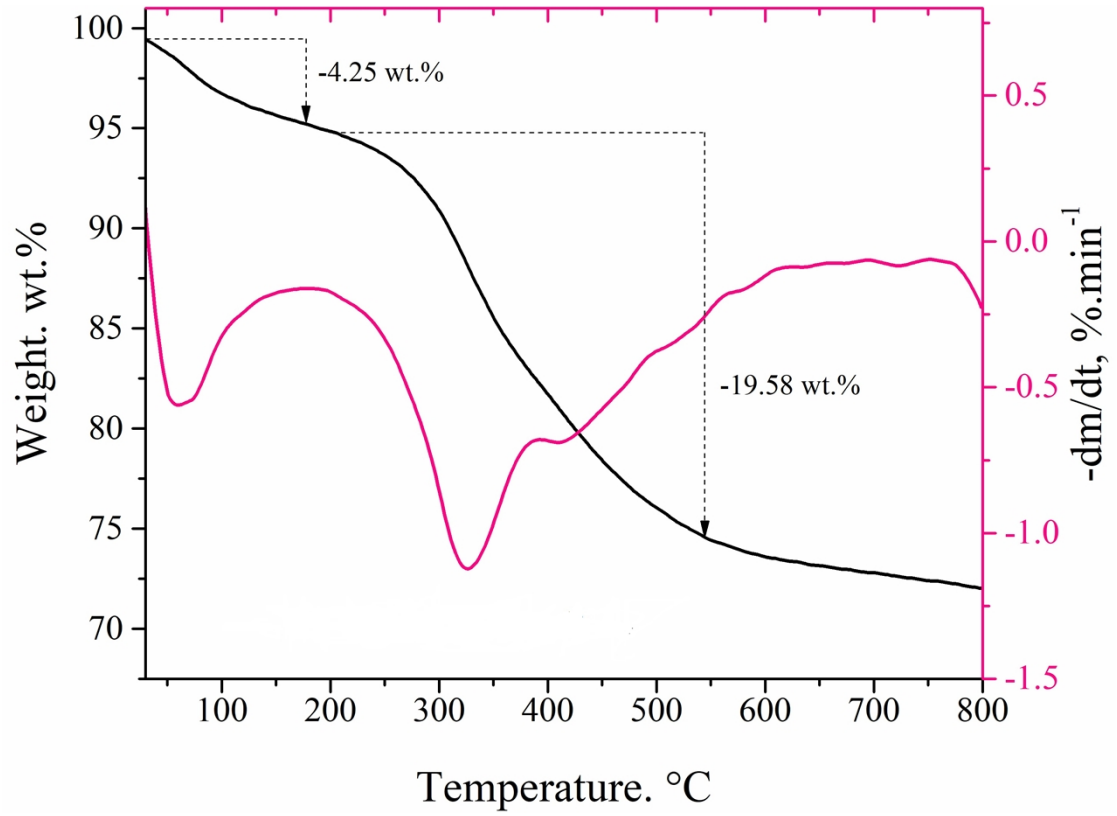

Figure S21:TG analysis of Re- Fe_3O_4@SiO_2-S-xIm$^+$$HSO_4^-$

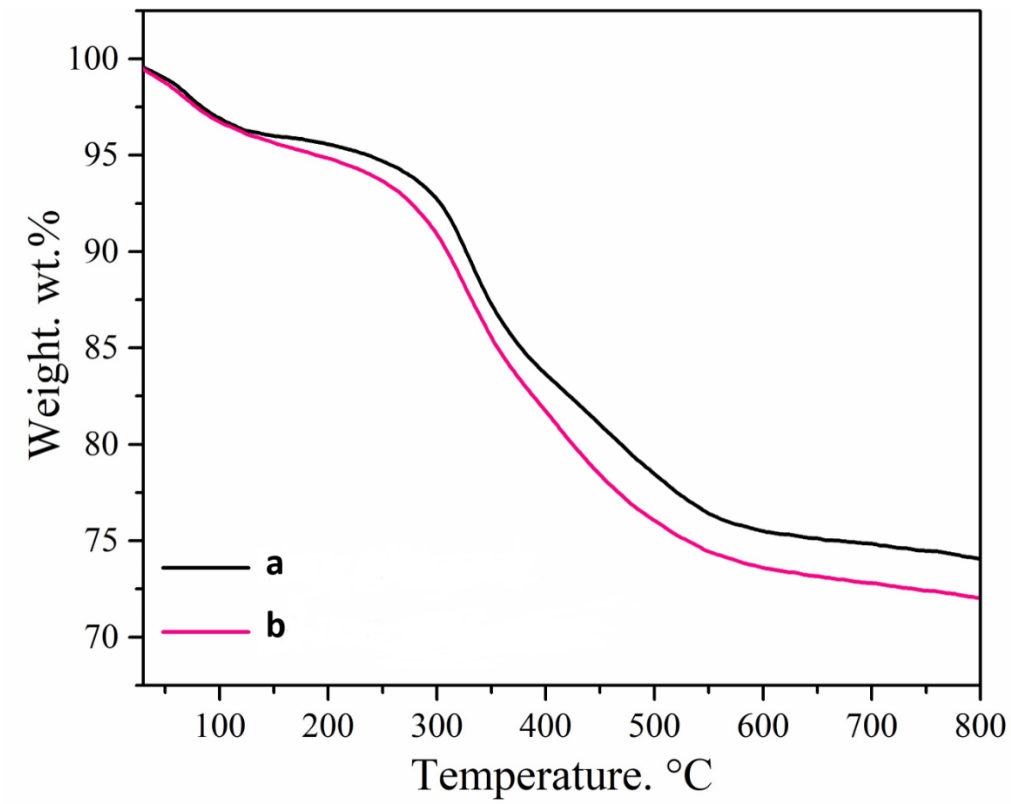

Figure S22: Comparison of TG analysis of Fe_3O_4@SiO_2-S-xIm$^+HSO_4^-$ (a) and Re-Fe_3O_4@SiO_2-S-xIm$^+HSO_4^-$ (b)

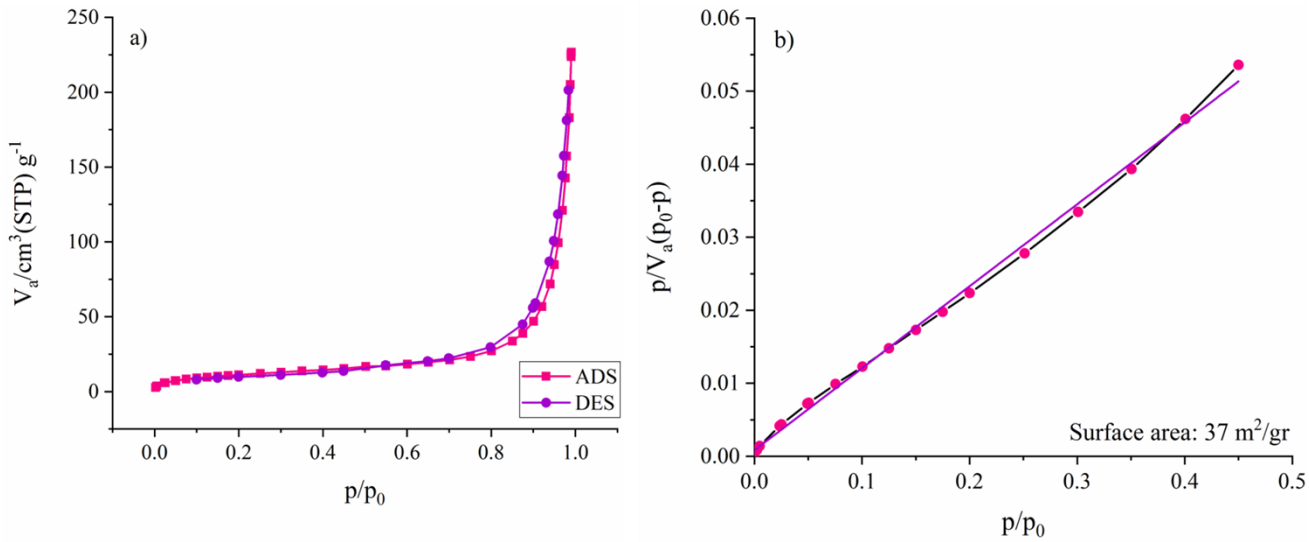

Figure S23: Nitrogen adsorption-desorption (a, BET isotherm of Re-Fe_3O_4@SiO_2-S-xIm$^+HSO_4^-$

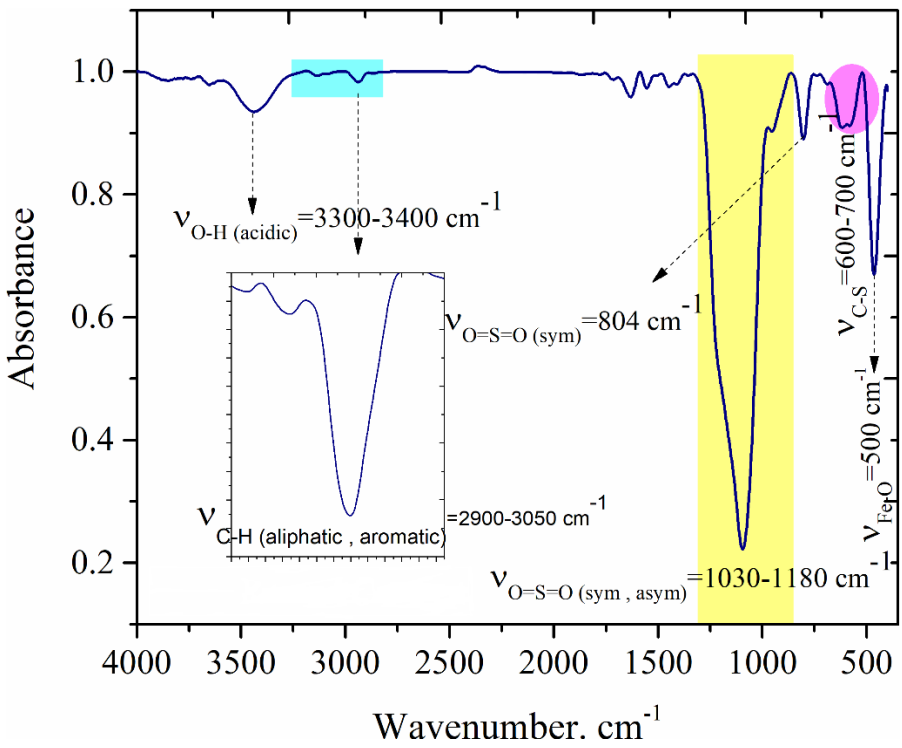

Figure S24: FT-IR spectra for Re-Fe_3O_4@SiO_2-S-xIm$^+$$HSO_4^-$

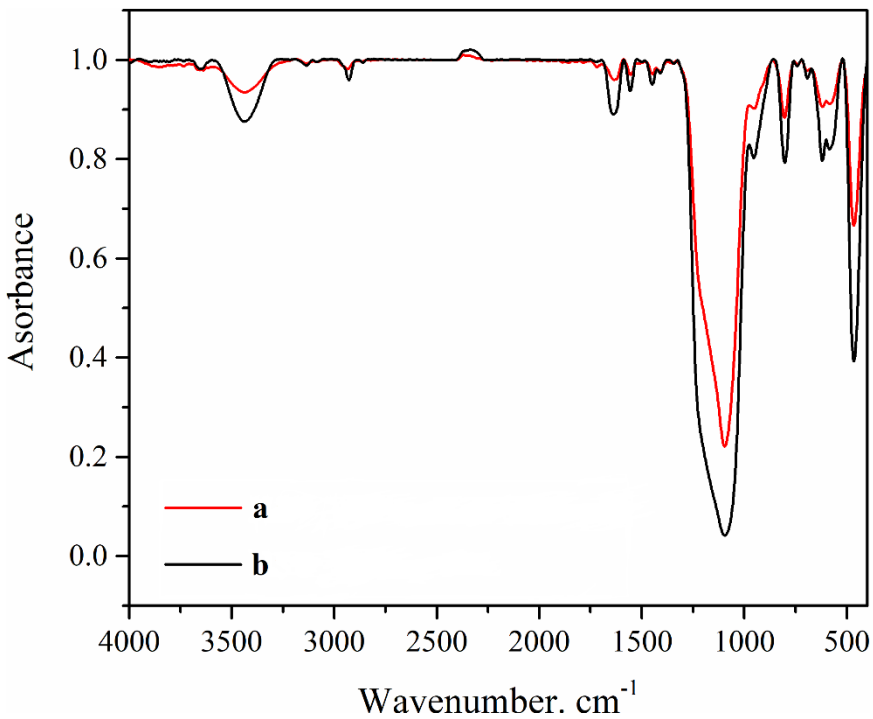

*Figure **S25:** Competition FT-IR spectra of Re-Fe_3O_4@SiO_2-S-xIm$^+$$HSO_4^-$ (a) with Fe_3O_4@SiO_2-S-xIm$^+$$HSO_4^-$ (b)*

Table S4: CHNS analysis of fresh catalyst and 10 turn reused catalyst

Sample	S (%)	H (%)	N (%)	C (%)	Loading of acidic group
$Fe_3O_4@SiO_2$-S-xIm$^+HSO_4^-$	3.761	1.126	2.037	10.66	0.51 mmol/gr
Re- $Fe_3O_4@SiO_2$-S-xIm$^+HSO_4^-$	3.438	1.251	1.993	11.21	0.41 mmol/gr

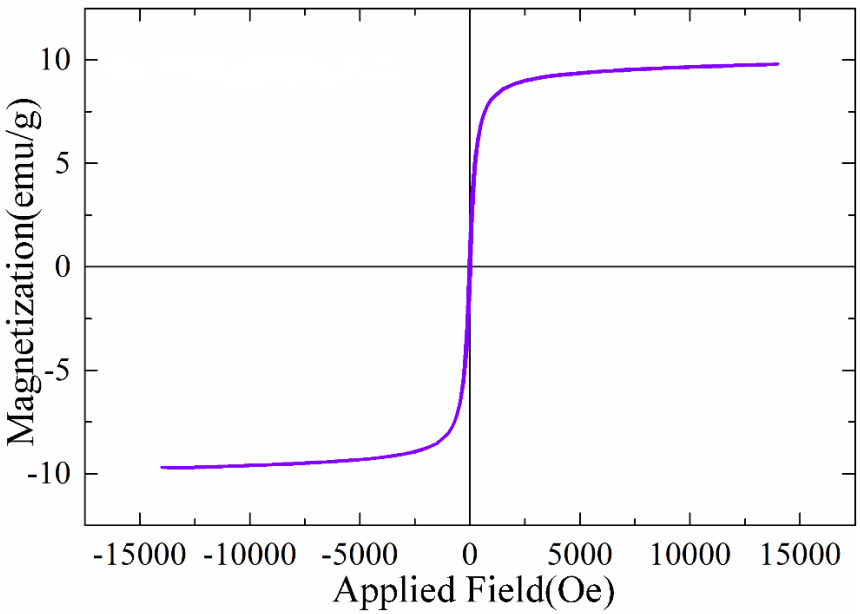

Figure S26:. The VSM curves of Re-$Fe_3O_4@SiO_2$-S-xIm$^+HSO_4^-$

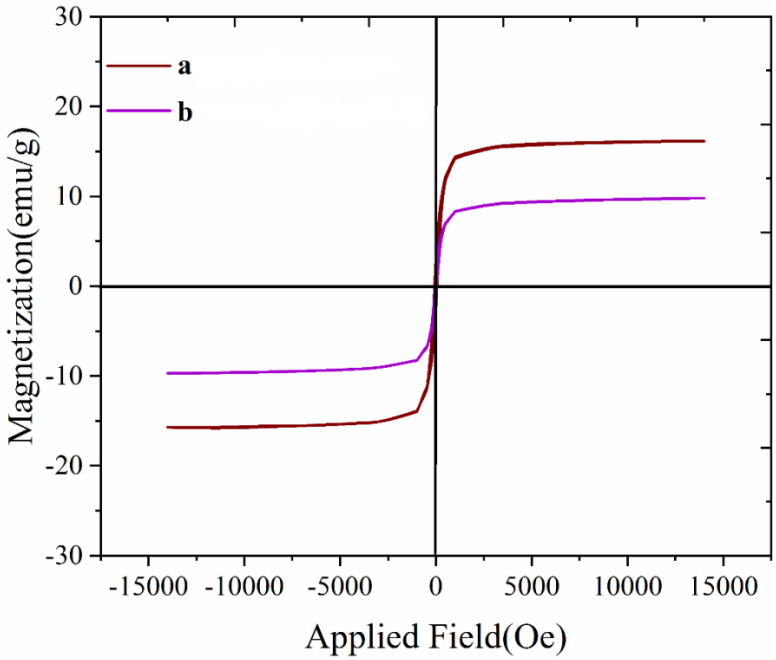

Figure S27: Competition VSM curves of $Fe_3O_4@SiO_2$-S-xIm$^+HSO_4^-$ (a) and Re-$Fe_3O_4@SiO_2$-S-xIm$^+HSO_4^-$ (b)

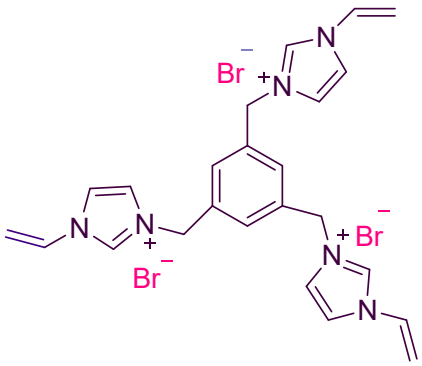

White powder, ^{1}H NMR (400MHz, DMSO) δ_H = 9.90 (s, 1H), 8.33 (s, 1H), 8.07 (s, 1H), 7.72 (s, 1H), 7.41 (dd, 1H), 6.06 (d, 1H), 5.56 (s, 2H), 5.46 (d.d, 1H), 2.52 (s, 2H): ^{13}C NMR (101 MHz, DMSO) δ_c= 136.21, 129.85, 129.33, 123.90, 119.88, 109.44, 52.07, 40.00.

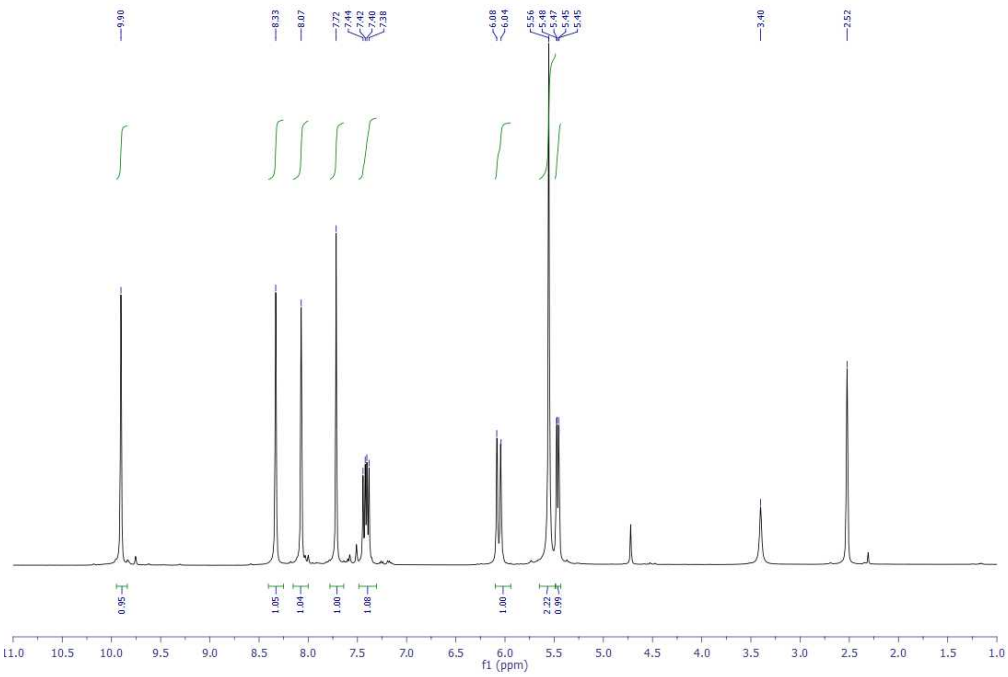

Figure S28: ^{1}H-NMR spectrum (400 MHz, DMSO-d_6) of 1,3,5-tris(vinylimidazolemethyl)benzene bromide ionic liquid

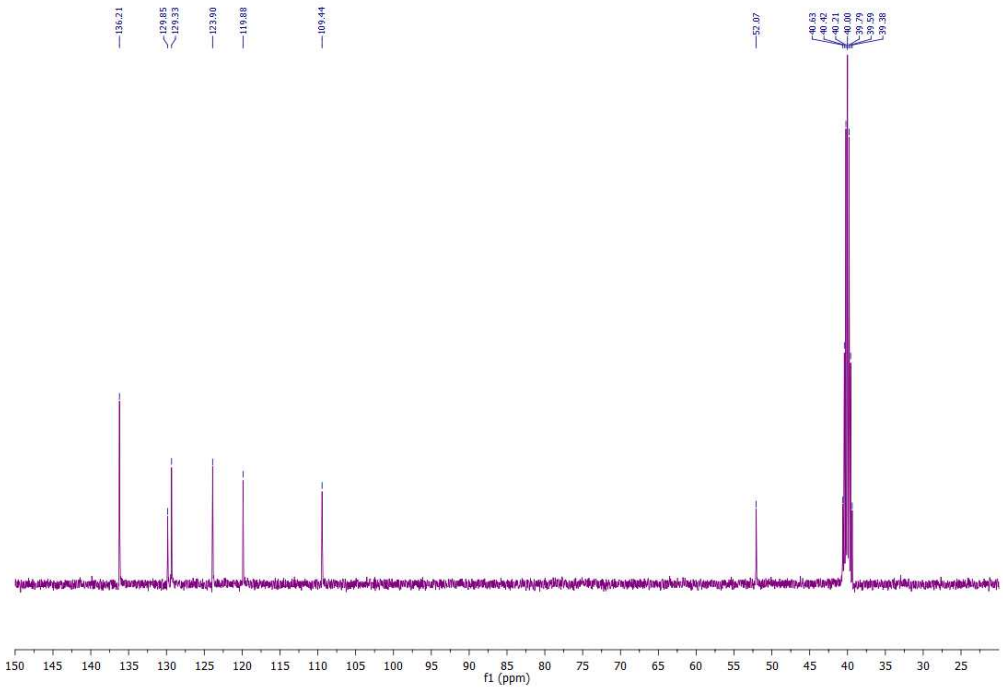

Figure S29: ^{13}C-NMR spectrum (100 MHz, DMSO-d_6) of 1,3,5-tris(vinylimidazolemethyl)benzene bromide ionic liquid

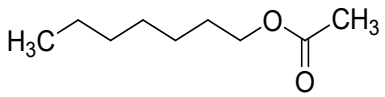

^{1}H NMR (400 MHz; $CDCl_3$): δ_H = 4.09 (t, 2H), δ_H = 2.04 (d, 3H), δ_H = 1.62 (s, 2H), δ_H = 1.30 (d, 6H), δ_H = 0.88 (s, 3H); ^{13}C NMR (100 MHz; $CDCl_3$): δ_C = 171.17, 64.61, 32.70, 28.90, 28.59, 25.85, 25.55, 20.96, 14.02.

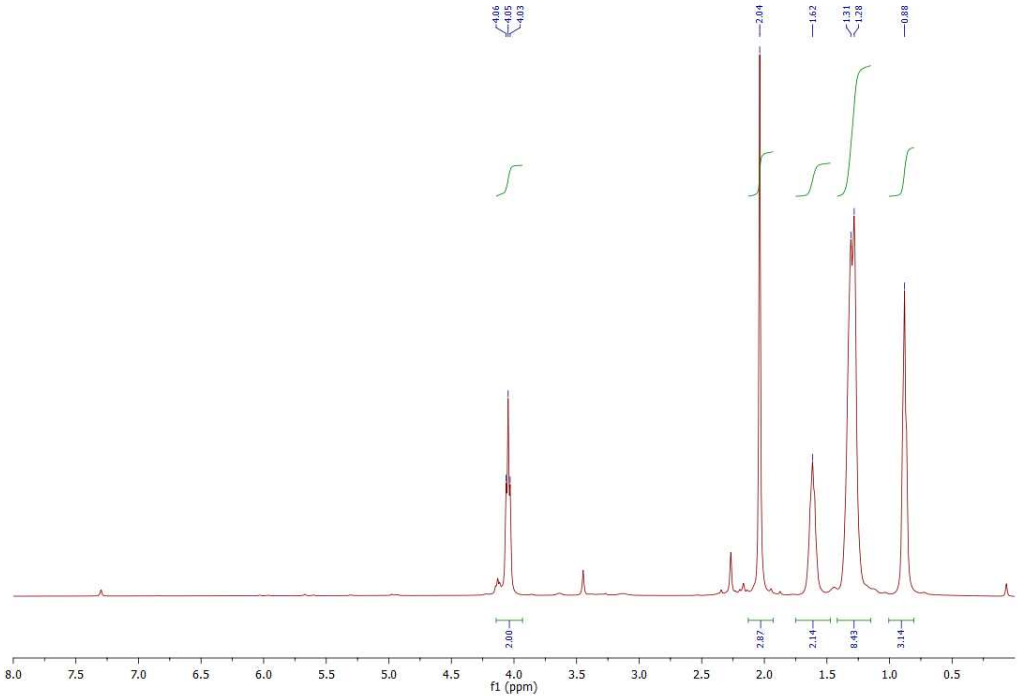

*Figure S**30:** ^{1}H-NMR spectrum (400 MHz, $CDCl_3$) of heptyl acetate*

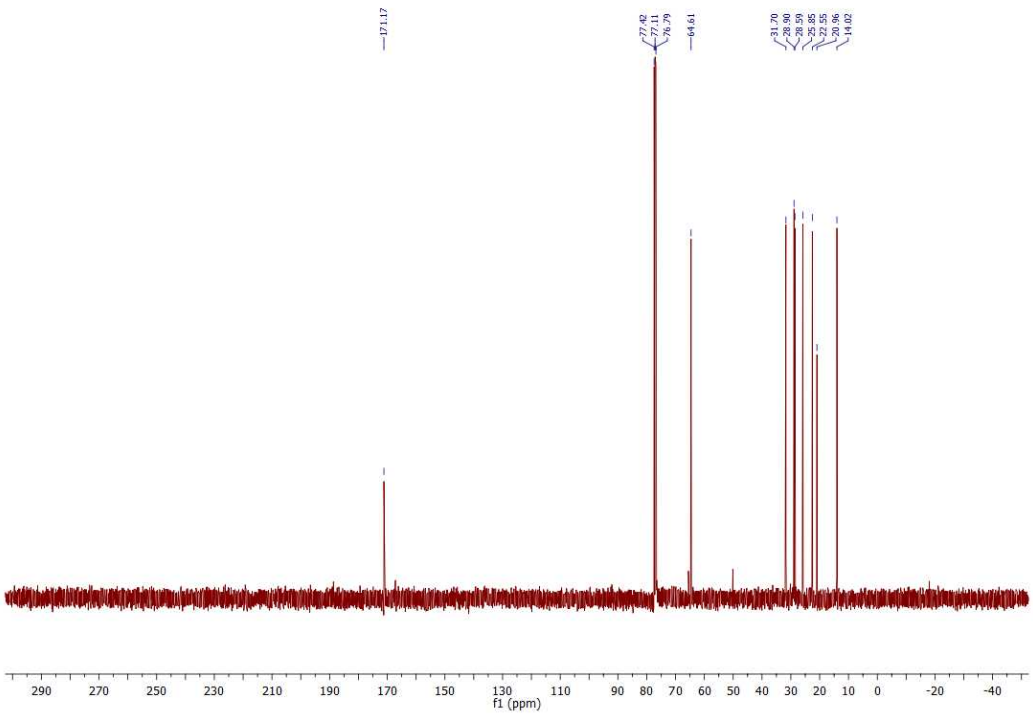

Figure S31: ^{13}C-NMR spectrum (100 MHz, $CDCl_3$) of heptyl acetate

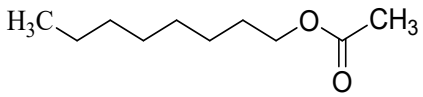

^{1}H NMR (400 MHz; $CDCl_3$): δ_H = 4.06 (t, 2H), δ_H = 2.01 (s, 3H), δ_H = 1.60 (m, 2H), δ_H = 1.25 (m, 2H), δ_H = 0.88 (t, 3H): ^{13}C NMR (100 MHz; $CDCl_3$): δ_C = 170.83, 64.59, 60.31, 31.73, 28.98, 28.41, 25.86, 22.58, 20.91, 14.30.

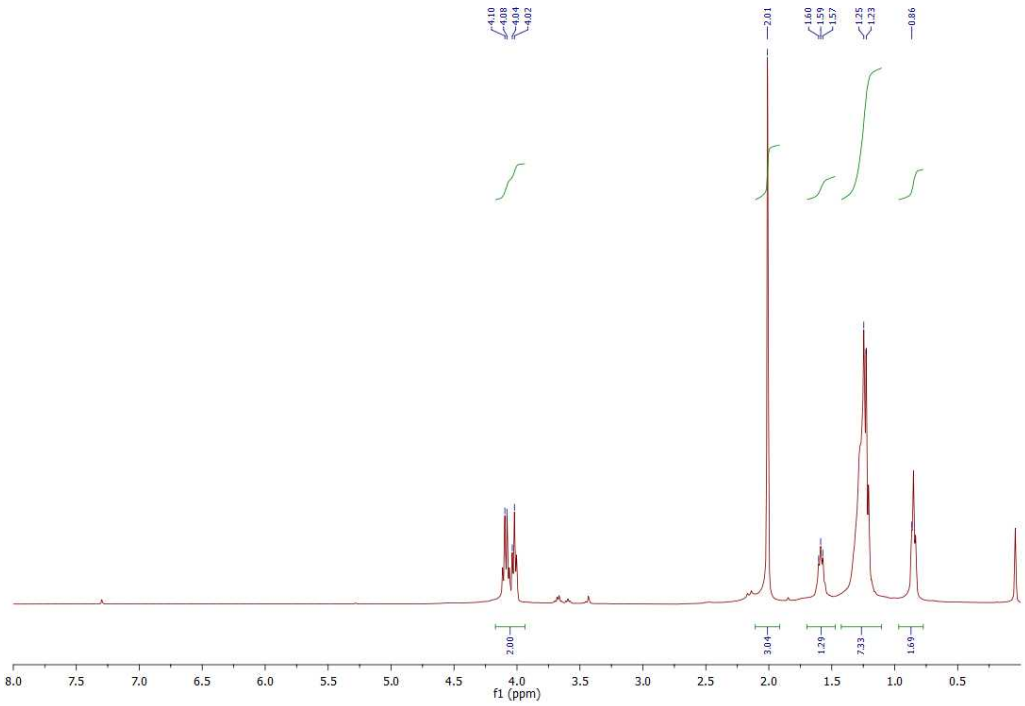

Figure S32: ^{1}H-NMR spectrum (400 MHz, $CDCl_3$) of octyl acetate

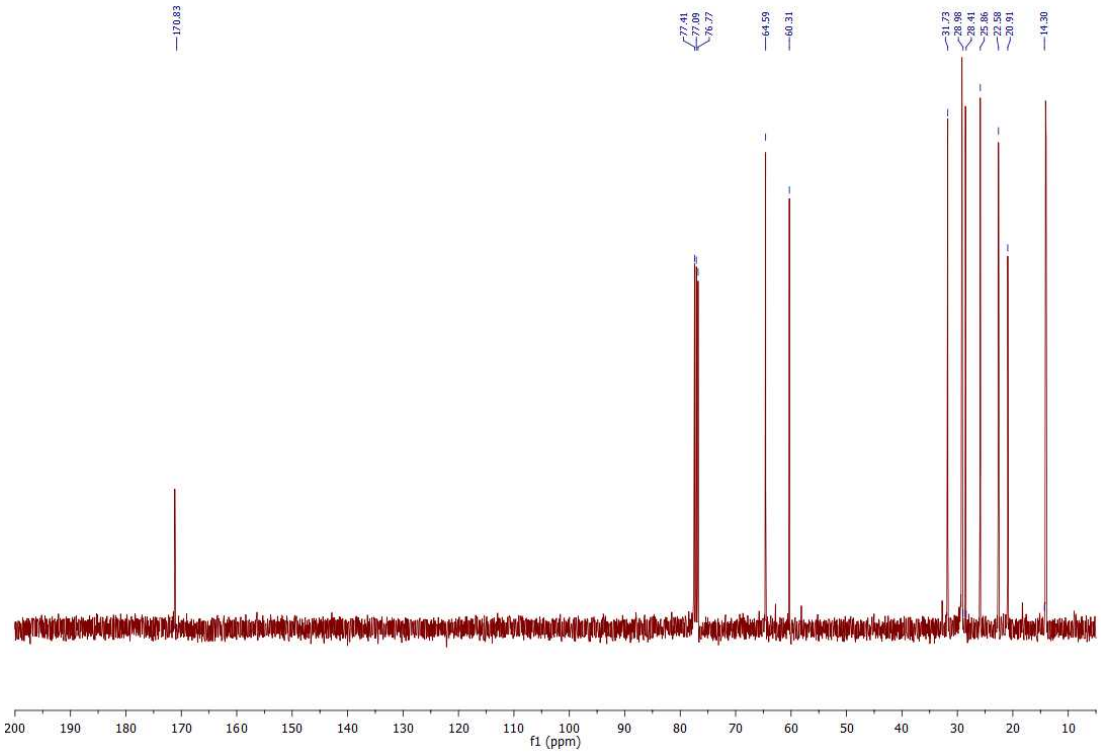

Figure S33: ^{13}C-NMR spectrum (100 MHz, $CDCl_3$) of octyl acetate

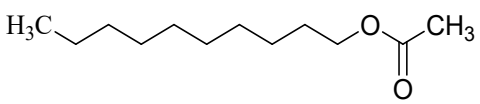

^{1}H NMR (400 MHz; $CDCl_3$): δ_H = 4.05 (t, 2H), δ_H = 2.02 (s, 3H), δ_H = 1.55-1.68 (m, 2H), δ_H = 1.10-1.49 (m,14H), δ_H = 0.86 (t, 3H); ^{13}C NMR (100 MHz; $CDCl_3$): δ_C = 171.15, 64.59, 53.36, 31.75, 29.49, 29.17, 28.59, 25.88, 25.84, 22.53, 20.88, 13.97.

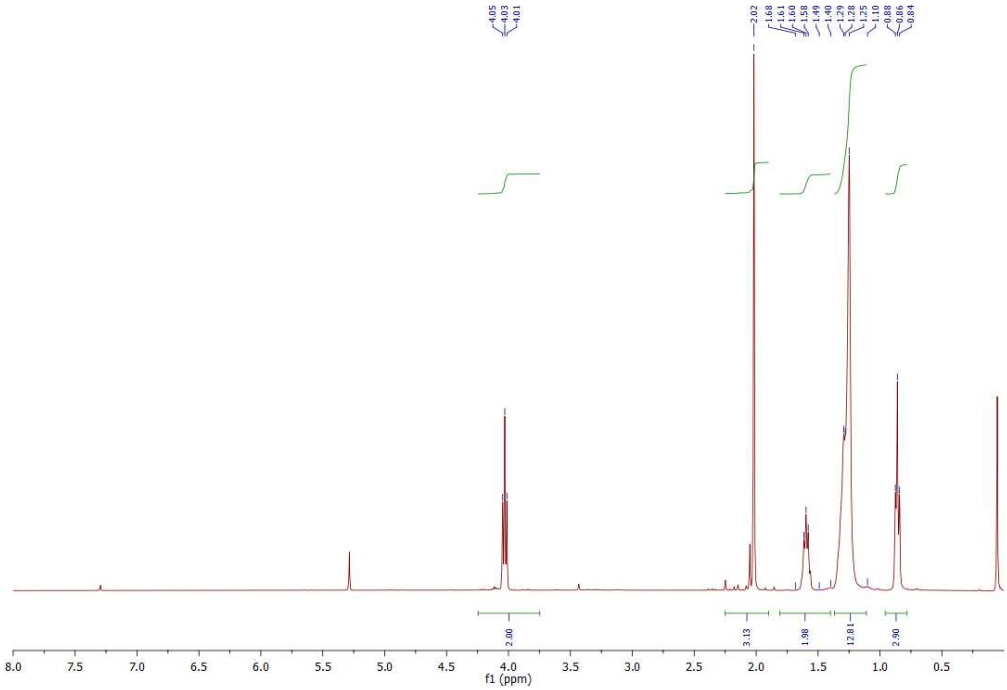

Figure S34: ^{1}H-NMR spectrum (400 MHz, $CDCl_3$) of decyl acetate

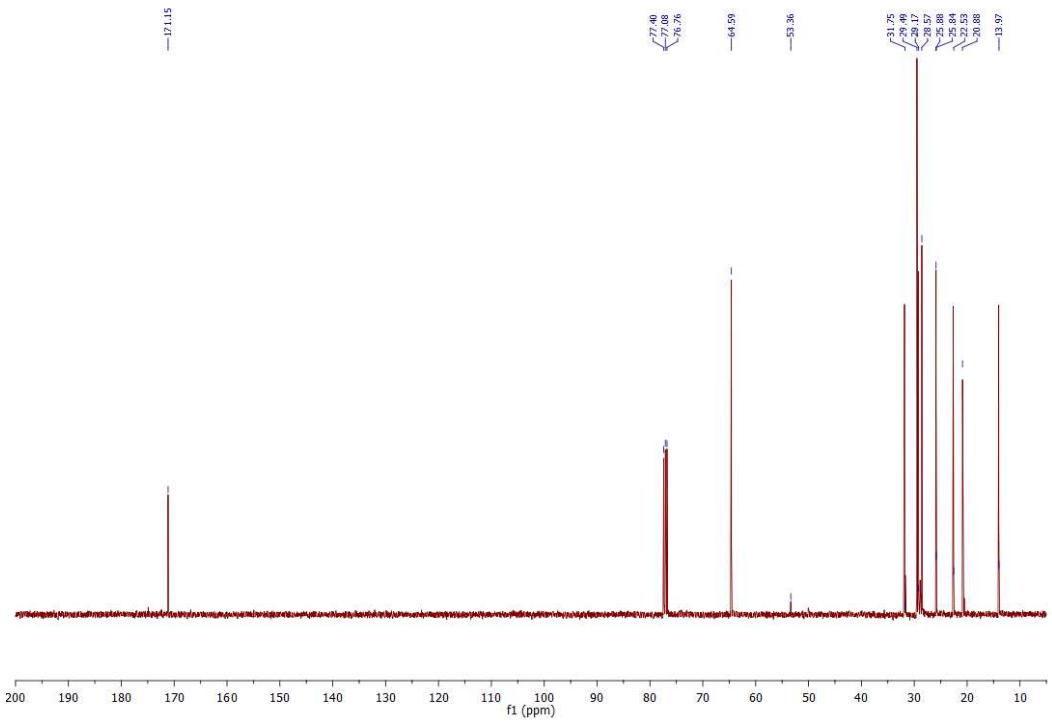

Figure S35: ^{13}C-NMR spectrum (100 MHz, $CDCl_3$) of decyl acetate

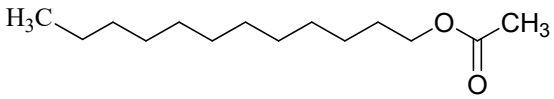

^{1}H NMR (400 MHz; $CDCl_3$): δ_H = 4.07 (t, 2H), δ_H = 2.06 (s, 3H), δ_H = 1.54-1-65 (m, 2H), δ_H = 1.14-1.42 (m, 18H), δ_H = 0.88 (t, 3H); ^{13}C NMR (100 MHz; $CDCl_3$): δ_C = 171.25, 64.67, 31.92, 29.65, 29.63, 29.58, 29.53, 29.35, 29.27, 28.61, 25.92, 22.69, 21.01, 14.11.

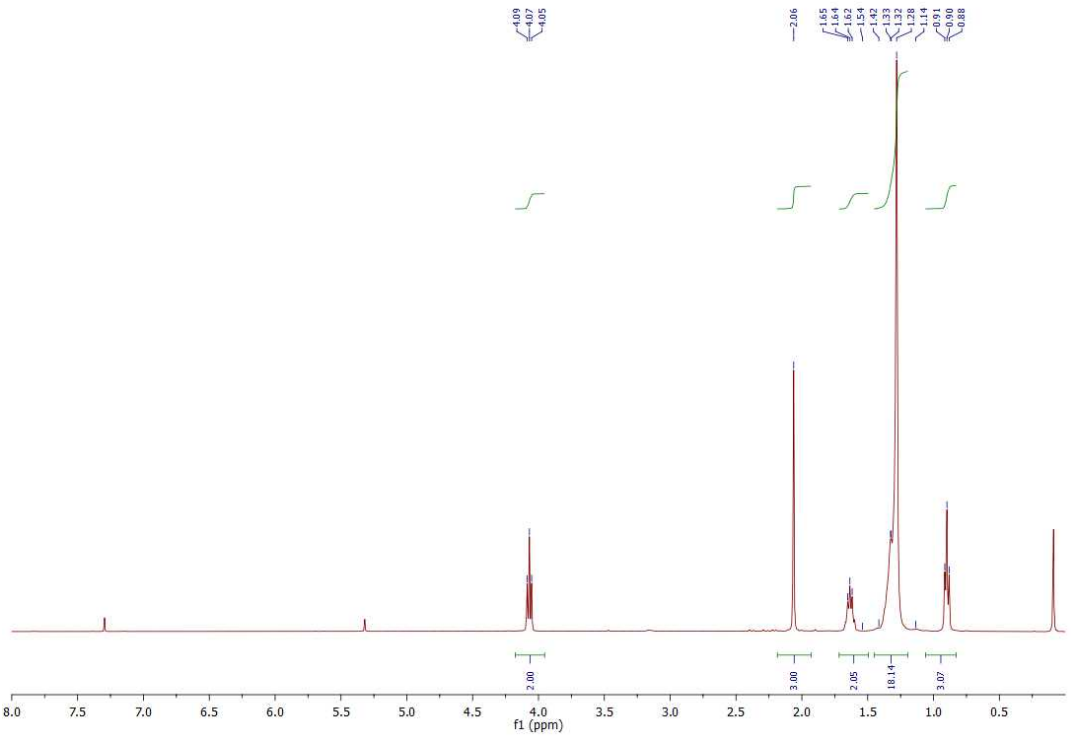

Figure S36: ^{1}H-NMR spectrum (400 MHz, $CDCl_3$) of dodecyl acetate

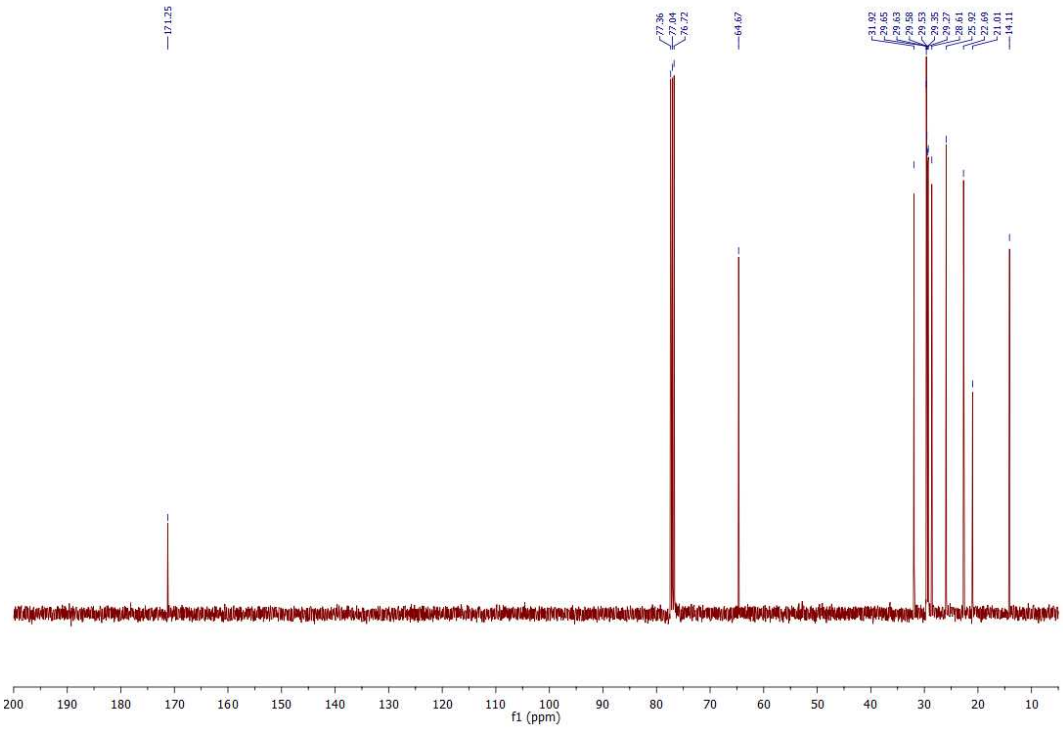

Figure S37: ^{13}C-NMR spectrum (100 MHz, $CDCl_3$) of dodecyl acetate

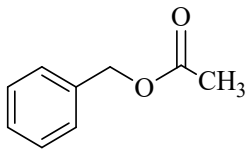

^{1}H NMR (400 MHz; $CDCl_3$): δ_H = 7.25-7.41 (m, 5H), δ_H = 5.16 (s, 2H), 2.15 (s, 3H); ^{13}C NMR (100 MHz; $CDCl_3$): δ_C = 170.92, 146.75, 136.99, 128.62, 128.32, 128.30, 126.99, 66.34, 21.04.

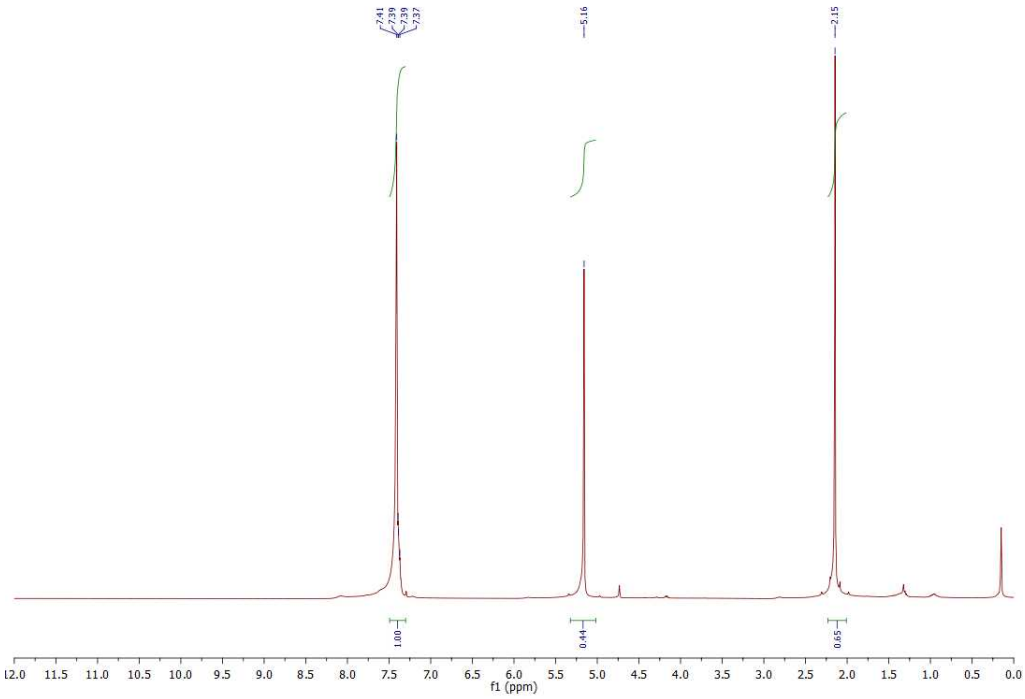

Figure S38: ^{1}H-NMR spectrum (400 MHz, $CDCl_3$) of benzyl acetate

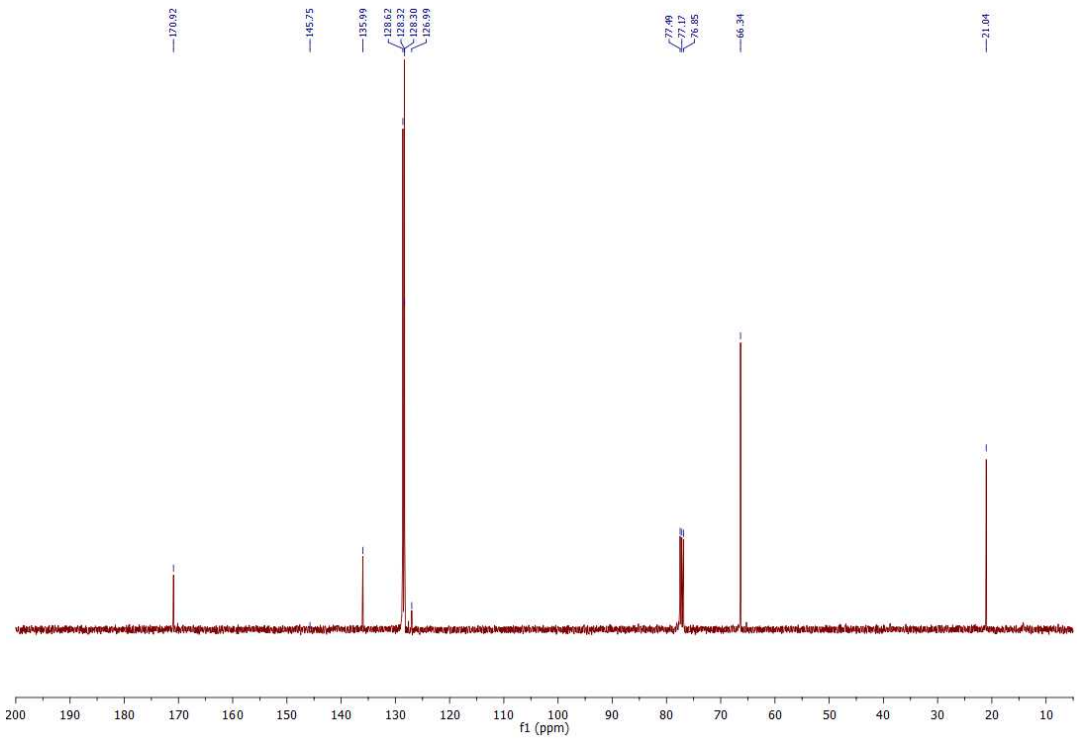

Figure S39: ^{13}C-NMR spectrum (100 MHz, $CDCl_3$) of benzyl acetate

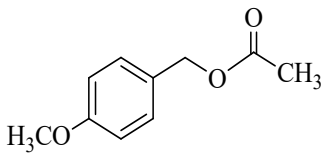

^{1}H NMR (400 MHz; $CDCl_3$): δ_H = 7.33 (d, H), δ_H = 6.92 (t, 2H), δ_H = 5.08 (s, 2H), δ_H = 3.81 (s, 3H); ^{13}C NMR (100MHz; $CDCl_3$): δ_C = 171.03, 159.72, 130.18, 129.46, 128.08, 114.16, 71.48, 66.17, 55.31, 21.11.

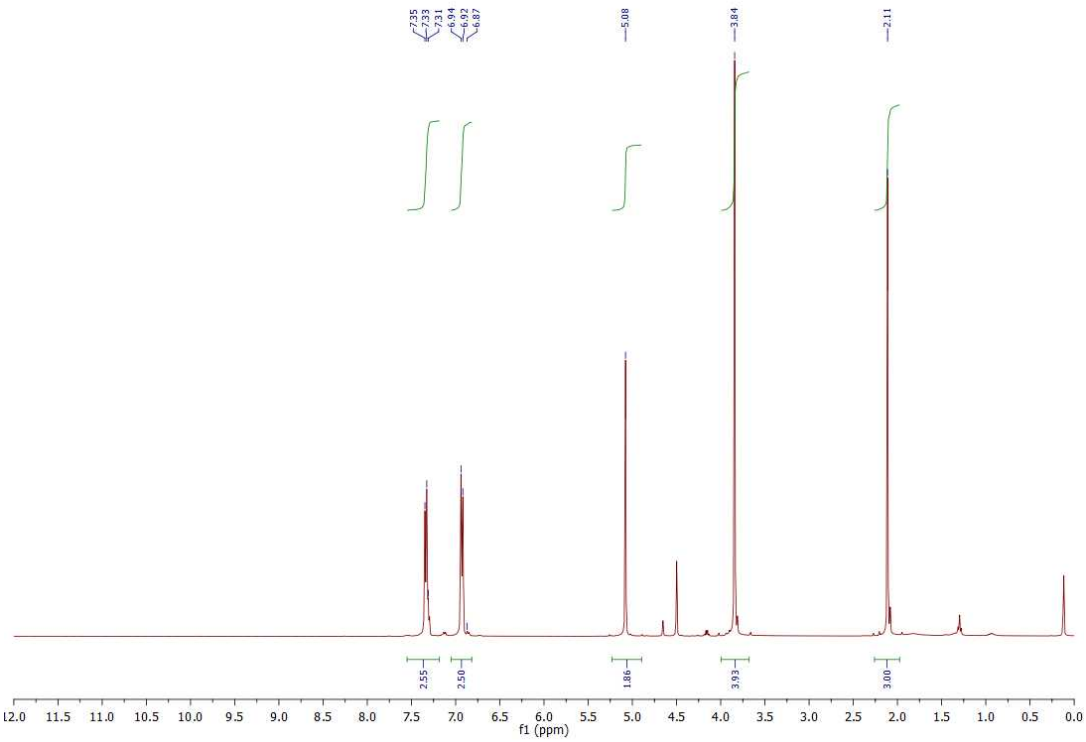

Figure S40: ^{1}H-NMR spectrum (400 MHz, $CDCl_3$) of 4-methoxybenzyl acetate

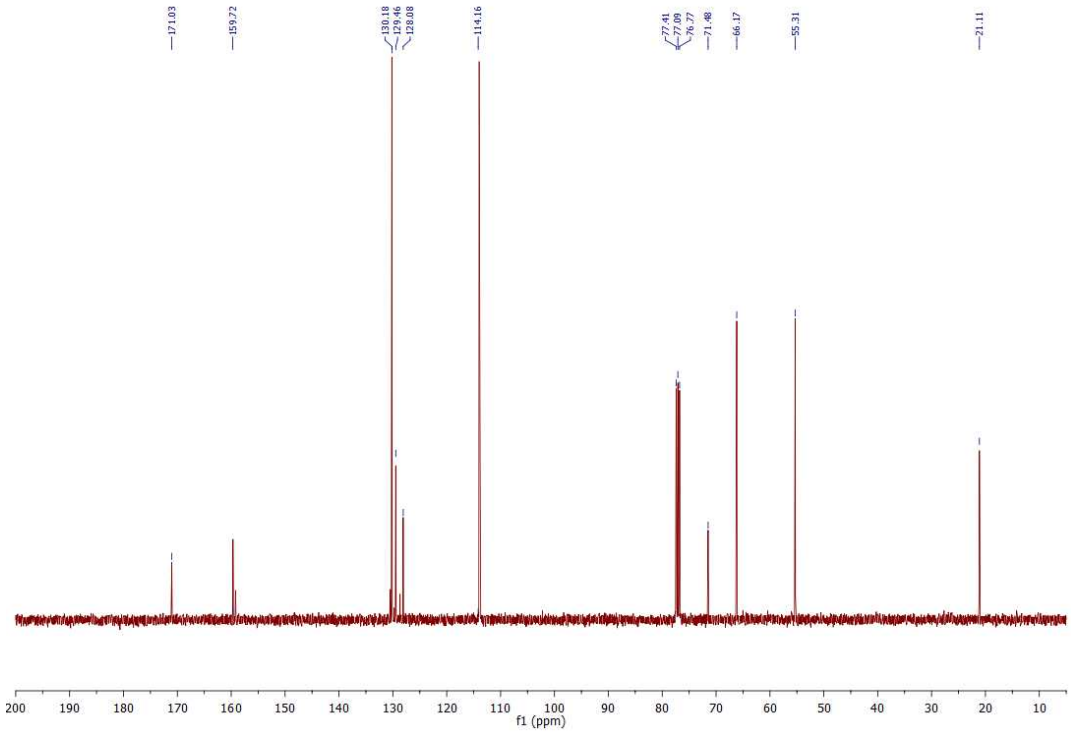

Figure S41: ^{13}C-NMR spectrum (100 MHz, $CDCl_3$) of 4-methoxybenzyl acetate

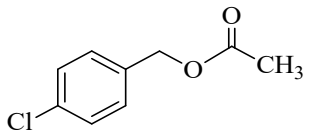

^{1}H NMR (400 MHz; $CDCl_3$): δ_H = 7.29- 7.36 (m, 4H), δ_H = 5.08 (s, 2H), δ_H = 2.11 (s, 3H); ^{13}C NMR (100 MHz; $CDCl_3$): δ_C = 170.84, 134.49, 134.13, 129.66, 128.76, 128.24, 65.48, 64.32, 20.95.

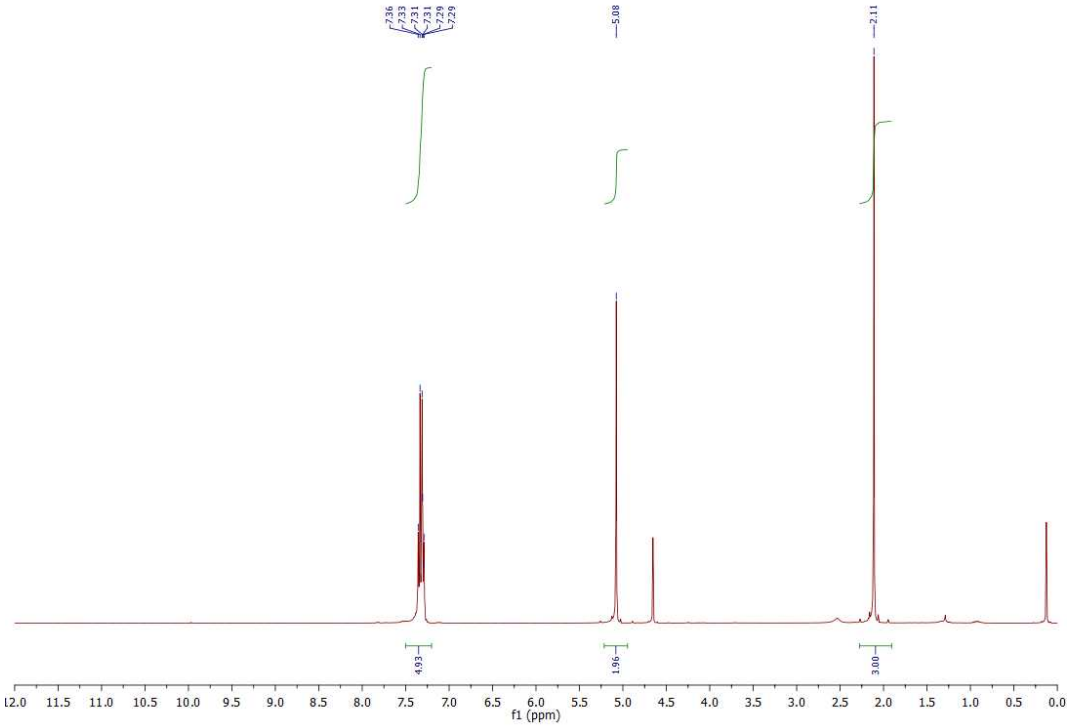

Figure S42: ^{1}H-NMR spectrum (400 MHz, $CDCl_3$) of 4-chlorobenzyl acetate

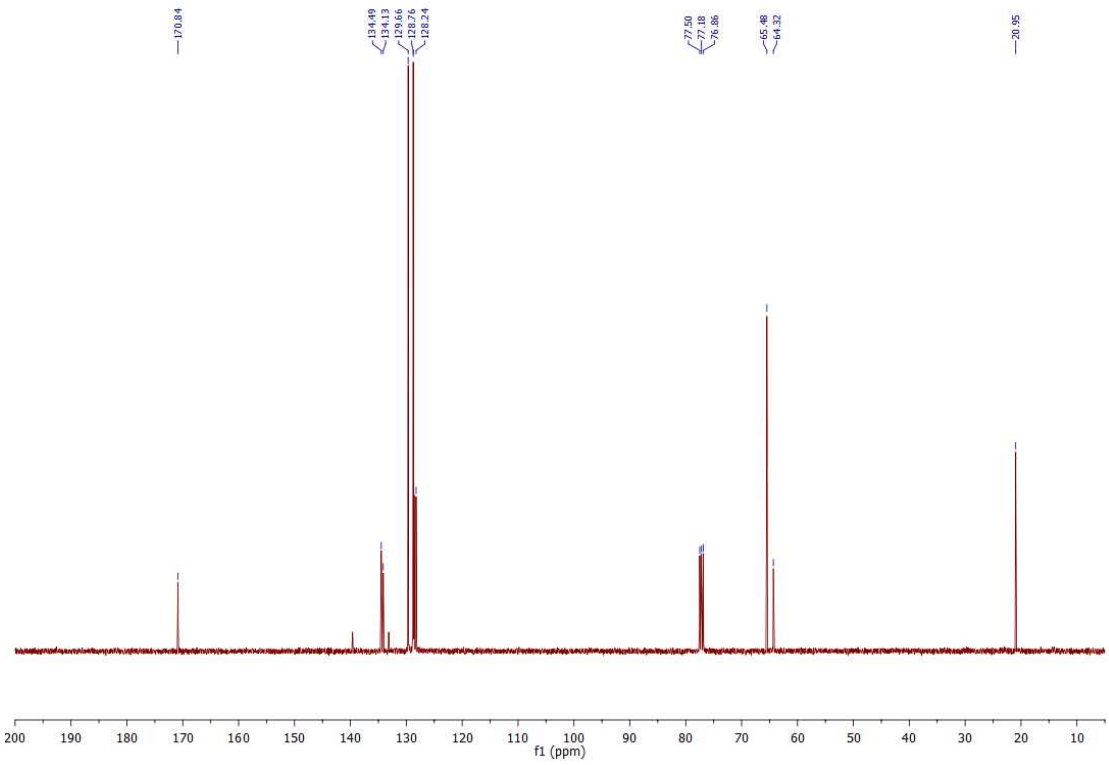

Figure S43: ^{13}C-NMR spectrum (100 MHz, $CDCl_3$) of 4-chlorobenzyl acetate

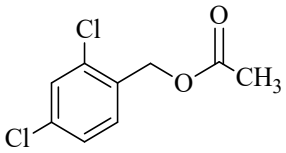

^{1}H NMR (400 MHz, $CDCl_3$); δ_H = 8.24 (d, 1H), δ_H = 7.57 (d.d, 2H), δ_H = 5.23 (s, 2H), δ_H = 2.18 (s, 3H): ^{13}C NMR (100 MHz, $CDCl_3$); δ_C = 170.57, 143.24, 128.40, 127.00, 123.81, 123.73, 64.79, 64.00, 20.85.

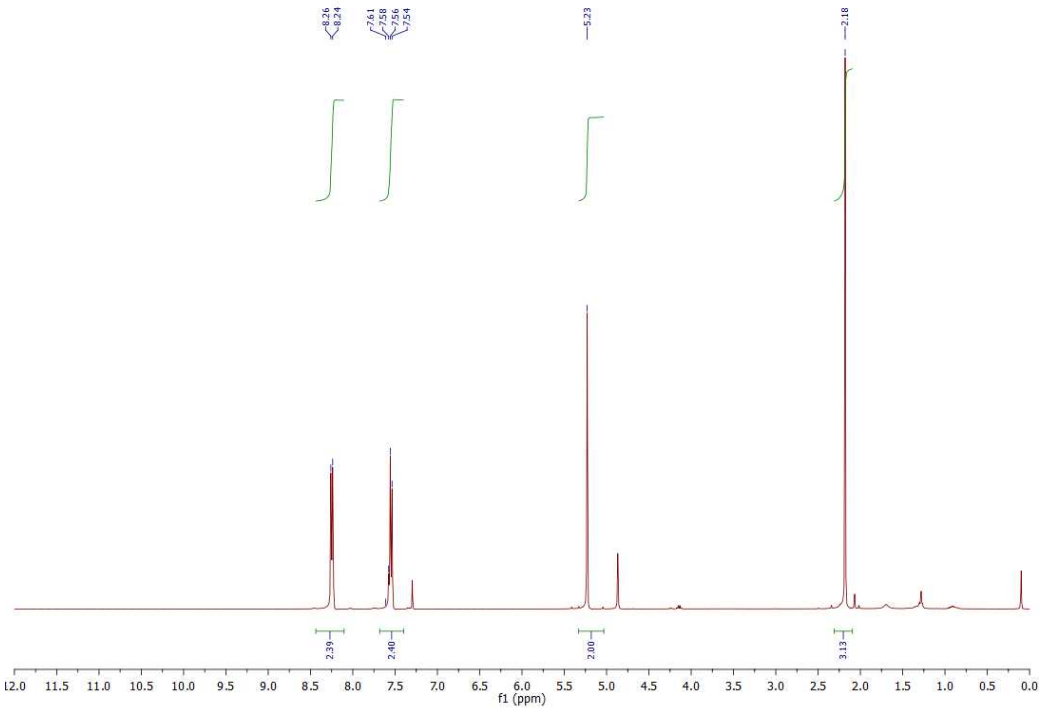

Figure S44: ^{1}H-NMR spectrum (400 MHz, $CDCl_3$) of 2,4-chlorobenzyl acetate

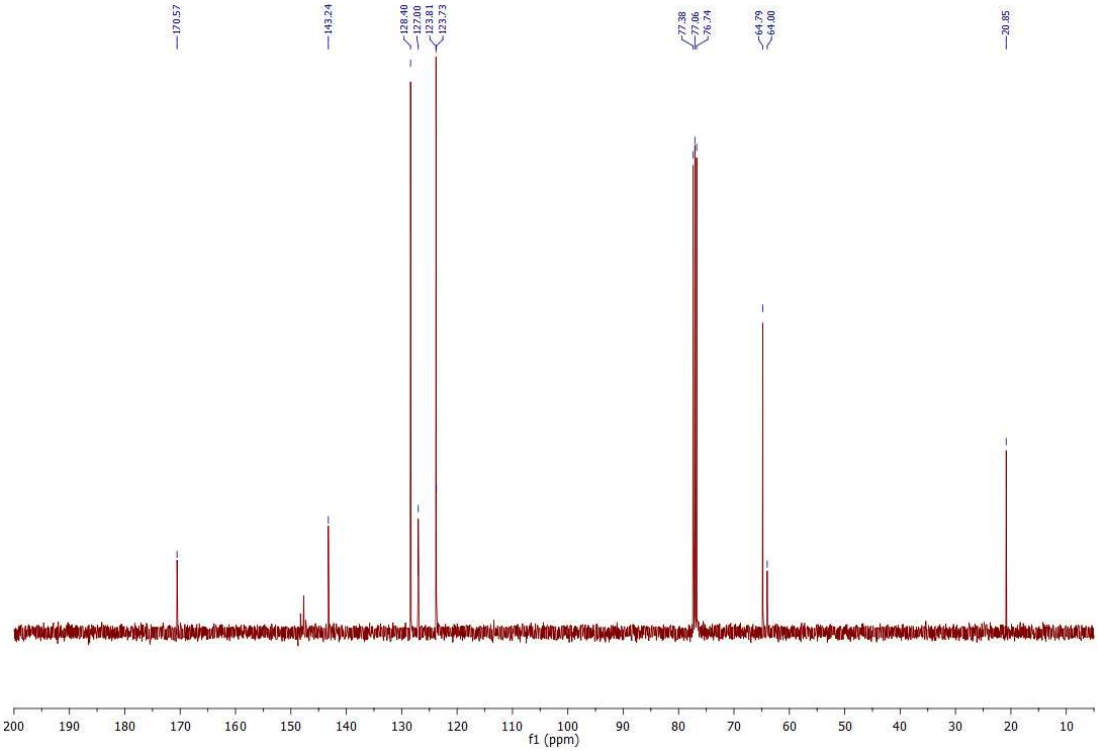

Figure S45: ^{13}C-NMR spectrum (100 MHz, $CDCl_3$) of 2,4-chlorobenzyl acetate

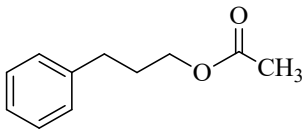

^{1}H NMR (400 MHz, $CDCl_3$); δ_H = 7.23-7-36 (m, 5H), δ_H = 4.12 (t, 2H), δ_H = 2.74 (q, 2H), δ_H = 2.10 (s, 3H), δ_H = 1.97-2.05 (m, 2H): ^{13}C NMR (100 MHz, $CDCl_3$); δ_C = 171.23, 140.98, 128.49, 128.44, 126.06, 63.95, 34.31, 31.96, 30.23, 20.99, 14.24.

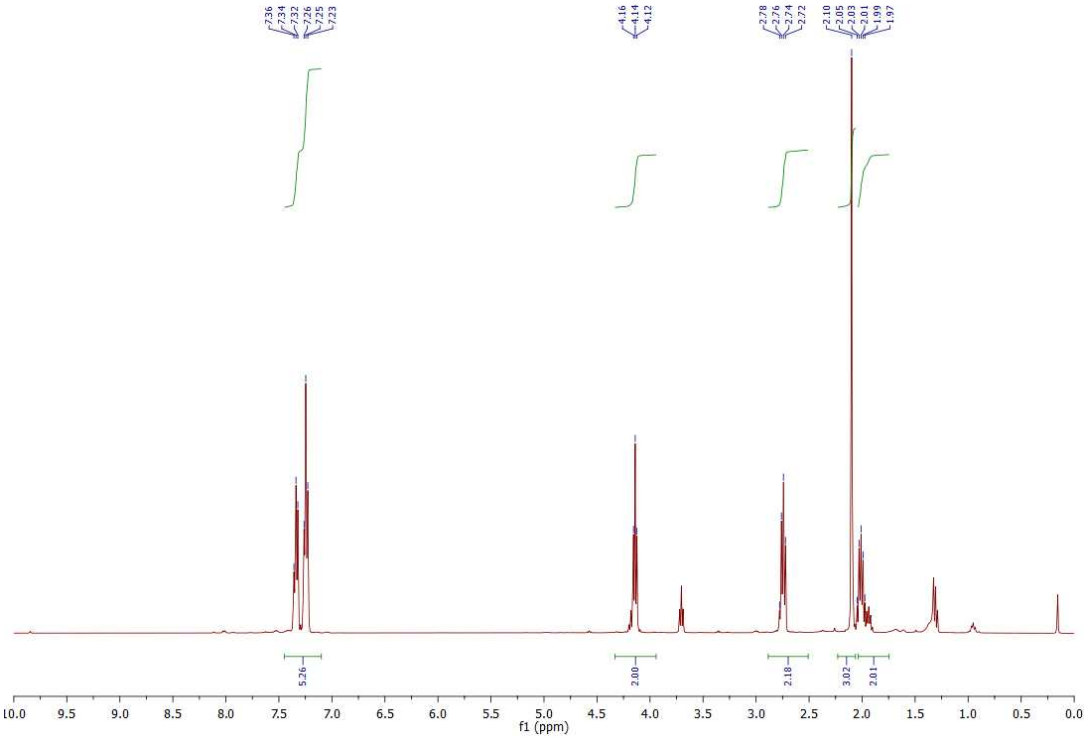

Figure S46: ^{1}H-NMR spectrum (400 MHz, $CDCl_3$) of 1-phenyl-3-propyl acetate

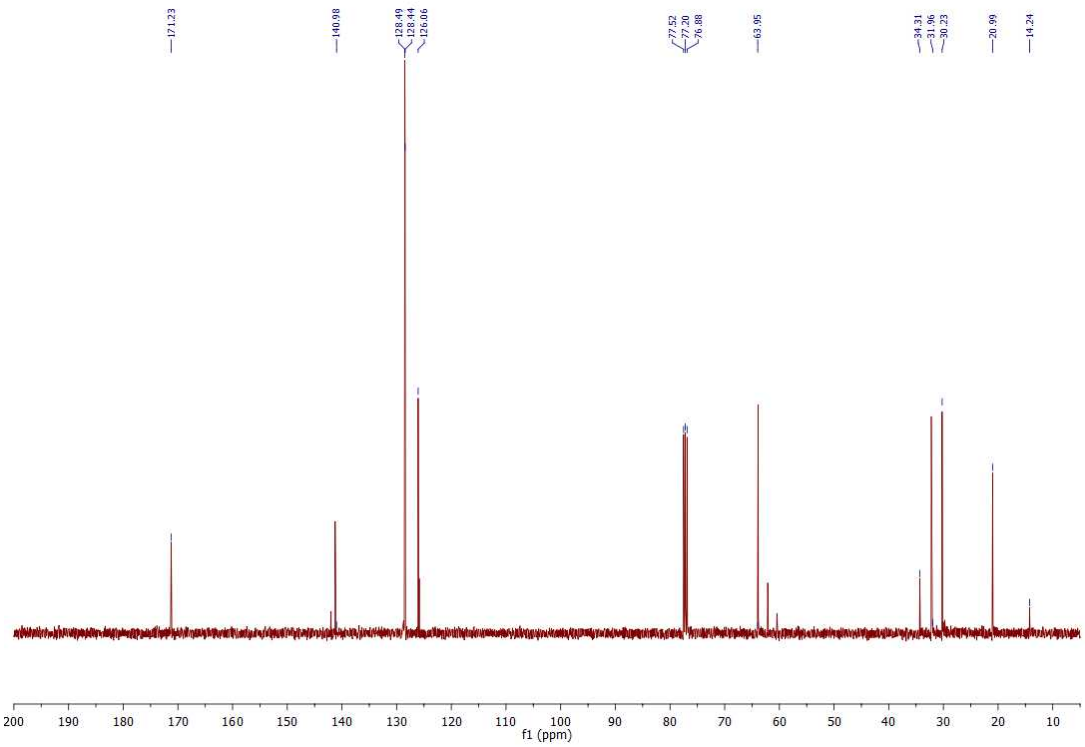

Figure S47: ^{13}C-NMR spectrum (100 MHz, $CDCl_3$) of 1-phenyl-3-propyl acetate

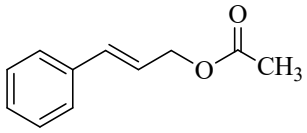

^{1}H NMR (400 MHz, $CDCl_3$); δ_H = 7.30-7.44 (m, 5H), δ_H = 6.67 (d, 1H), δ_H = 6.29-6.36 (m, 1H), δ_H = 4.76 (q, 2H), δ_H = 2.15 (s, 3H): ^{13}C NMR (100 MHz, $CDCl_3$); δC = 170.87, 136.22, 134.24, 128.04, 128.11, 126.64, 123.19, 65.11, 31.62, 21.03, 14.16.

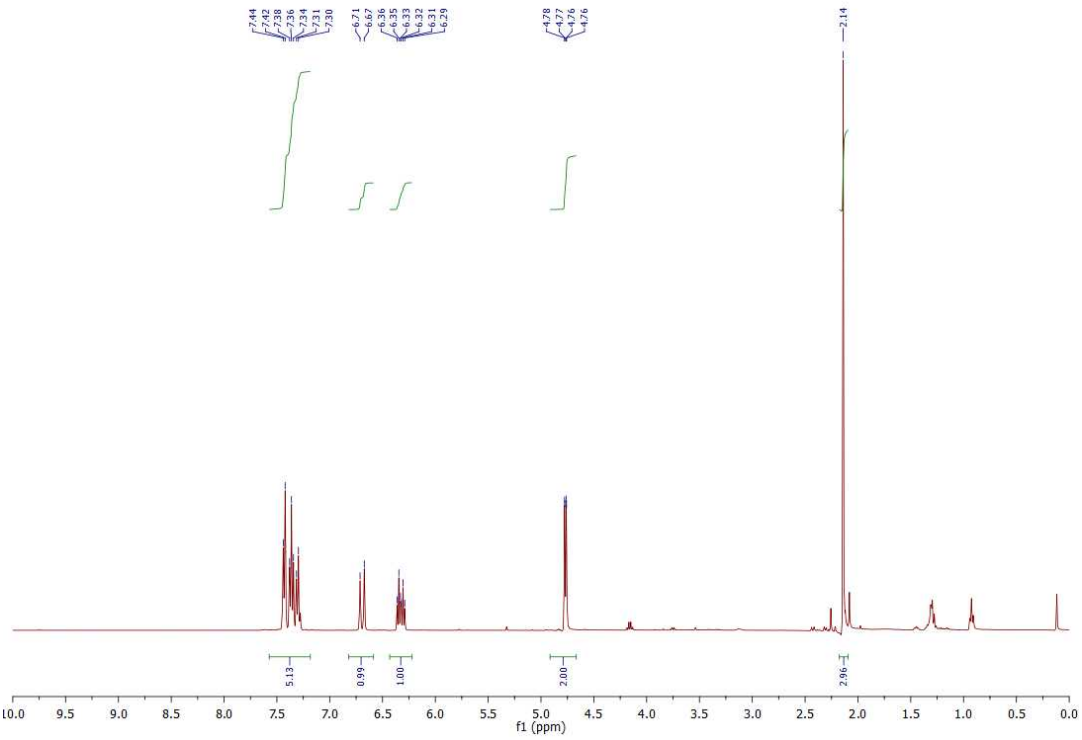

Figure S48: ^{1}H-NMR spectrum (400 MHz, $CDCl_3$) of cinnamyl acetate

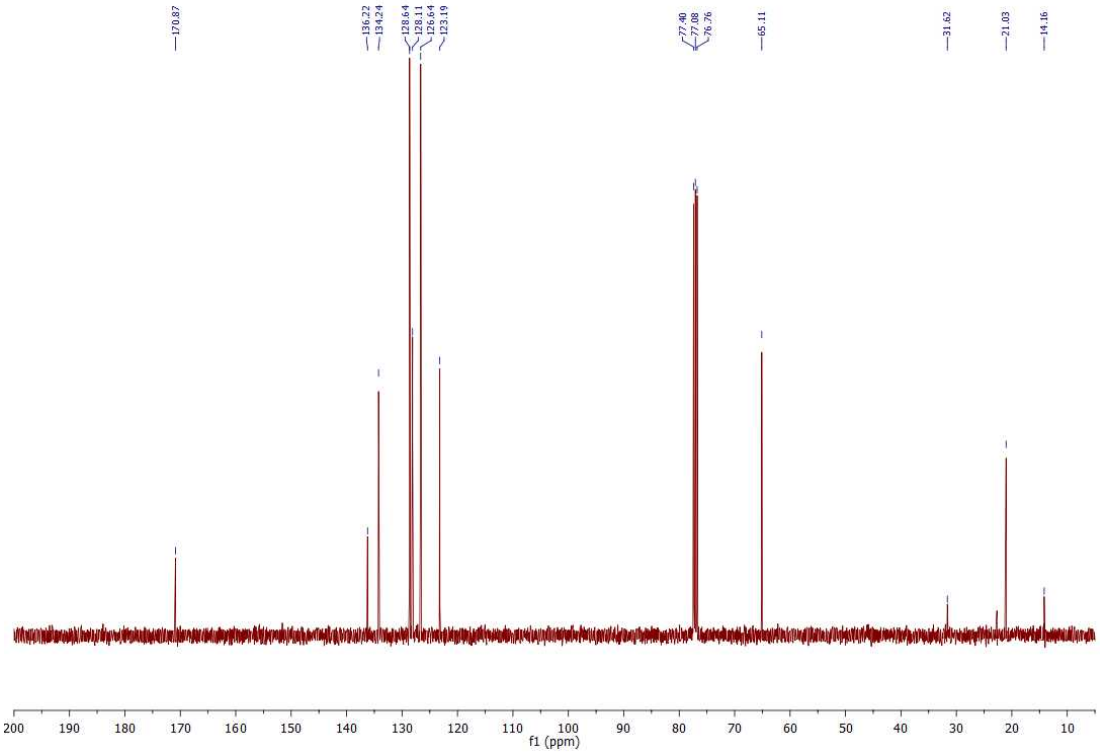

Figure S49: ^{13}C-NMR spectrum (100 MHz, $CDCl_3$) of cinnamyl acetate

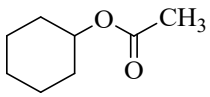

^{1}H NMR (400 MHz, $CDCl_3$); δ_H = 4.75 (m, 1H), δ_H = 2.03 (s, 3H), δ_H = 1.71-1.86-1.28 (m, 10H) ; ^{13}C NMR (100 MHz, $CDCl_3$); δC = 170.65, 77.43, 72.69, 31.64, 31.39, 25.36, 23.80, 23.27, 21.42.

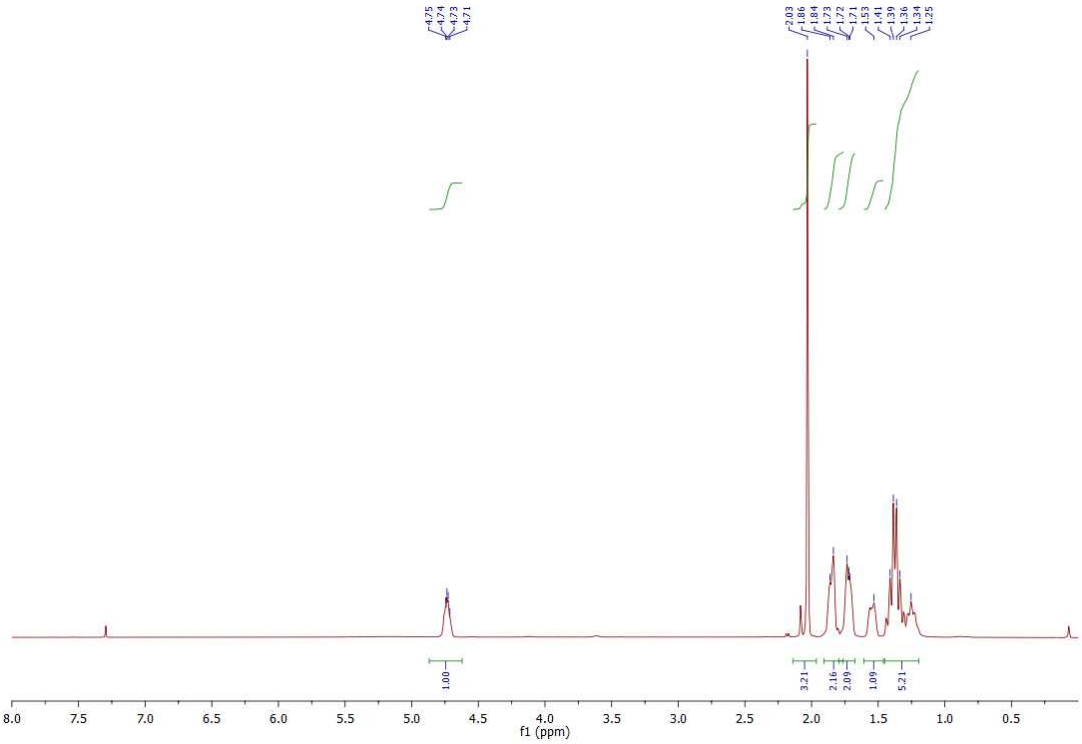

Figure S50: ^{1}H-NMR spectrum (400 MHz, $CDCl_3$) of cyclohexyl acetate

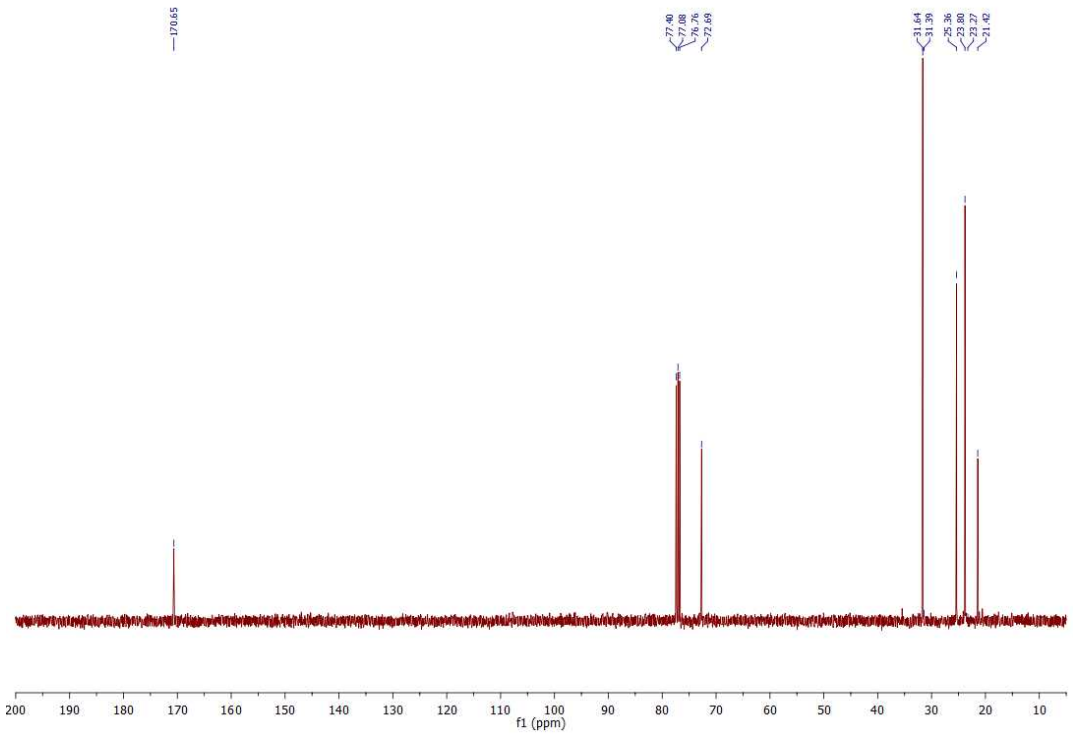

Figure S51: ^{13}C-NMR spectrum (100 MHz, $CDCl_3$) of cyclohexyl acetate

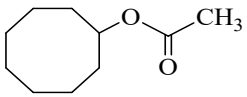

^{1}H NMR (400 MHz, $CDCl_3$); δ_H = 4.89- 4.95 (m, 1H), δ_H = 2.03 (s, 3H), δ_H = 1.88-1.94 (m, 4H), δ_H = 1.25-1.69 (m, 10H): ^{13}C NMR (100 MHz, $CDCl_3$); δC = 170.56, 75.18, 72.76, 37.80, 33.81, 28.28, 28.11, 22.87, 22.62, 21.51.

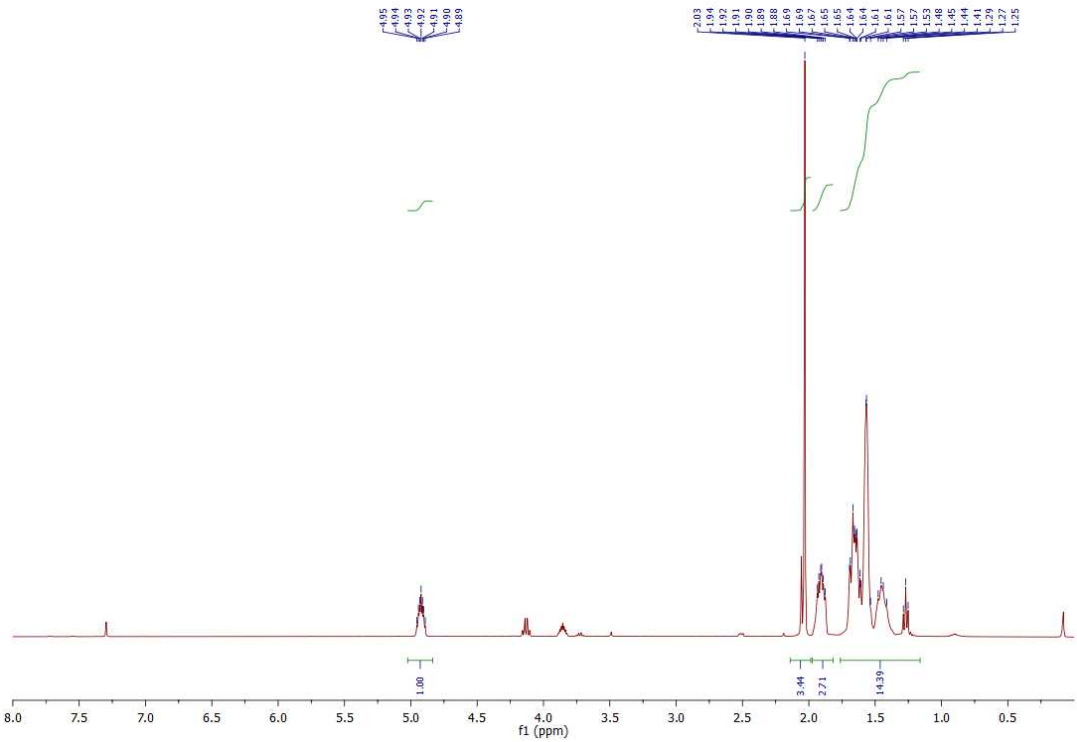

Figure S52: ^{1}H-NMR spectrum (400 MHz, $CDCl_3$) of cyclooctyl acetate

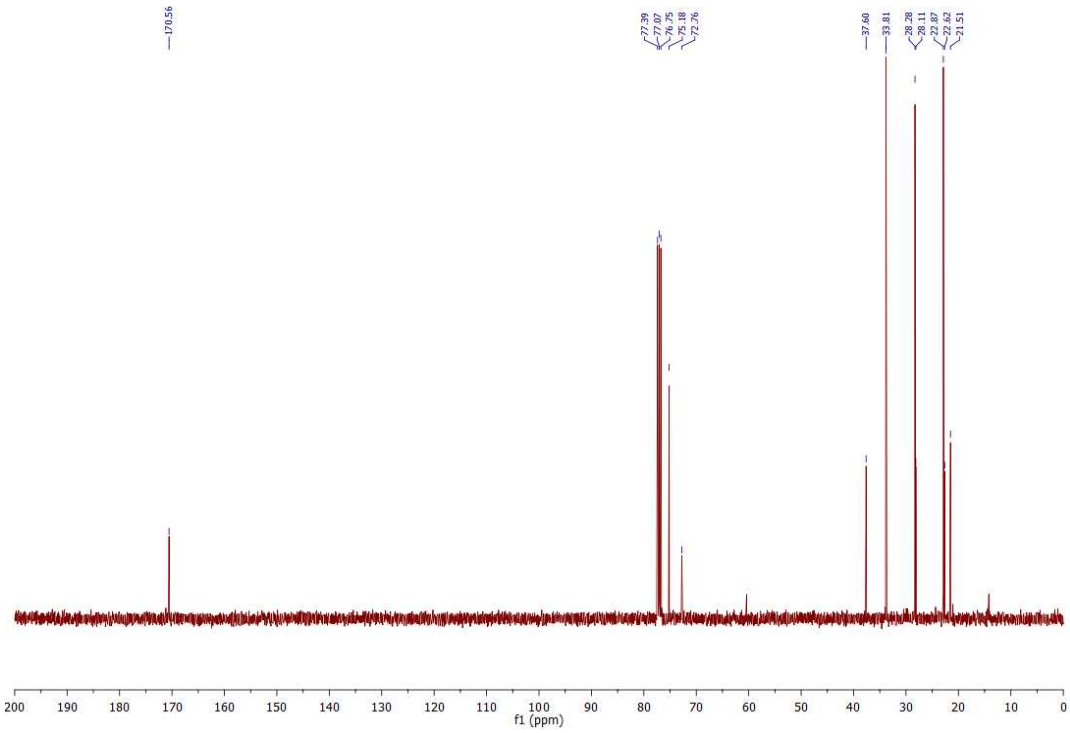

Figure S53: ^{13}C-NMR spectrum (100 MHz, $CDCl_3$) of cyclooctyl acetate

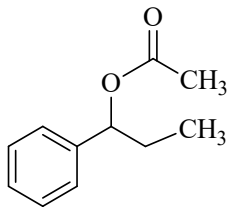

^{1}H NMR (400 MHz, $CDCl_3$); δ_H = 7.41 (t, 5H), δ_H = 5.73 (t, 2H), δ_H = 2.08 (s, 3H), δ_H = 1.79-1.99 (m, 2H), δ_H = 0.91-0.98 (m, 3H): ^{13}C NMR (100 MHz, $CDCl_3$); δC = 170.54, 144.69, 140.56, 128.41, 127.97, 126.34, 125.79, 31.67, 29.33, 21.29, 9.96.

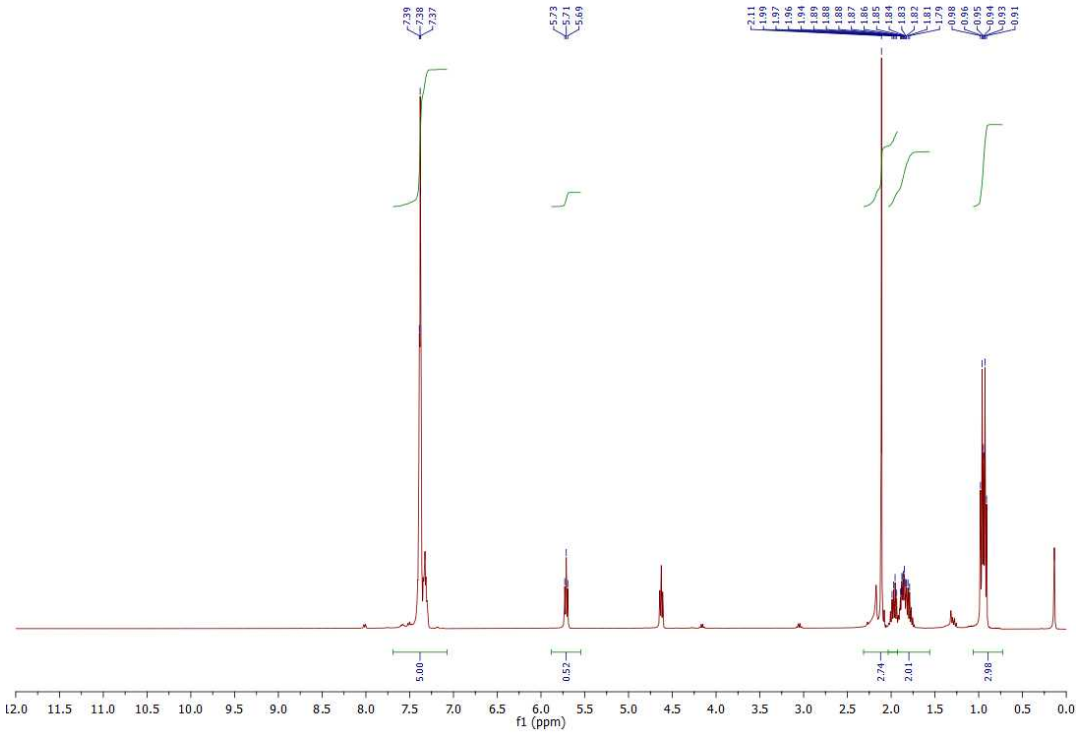

Figure S54: ^{1}H-NMR spectrum (400 MHz, $CDCl_3$) of 1-phenyl-1-propyl acetate

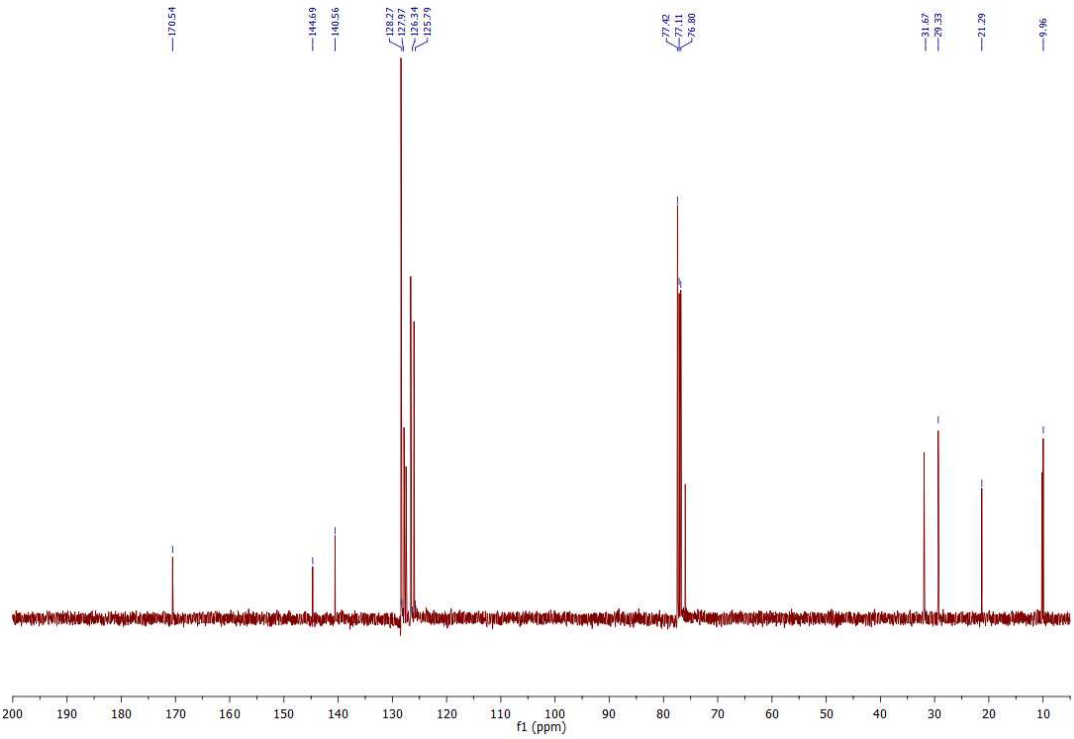

Figure S55: ^{13}C-NMR spectrum (100 MHz, $CDCl_3$) of 1-phenyl-1-propyl acetate

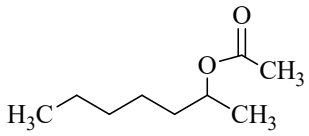

^{1}H NMR (400 MHz, $CDCl_3$); δ_H = 4.94 (q, 1H), δ_H = 2.05 (s, 3H), δ_H = 1.58 (s, 2H), δ_H = 1.22-1.50 (m, 9H), δ_H = 0.89 (d, 3H):): ^{13}C NMR (100 MHz, $CDCl_3$); δC = 170.86, 71.11, 68.21, 35.90, 31.65, 25.09, 22.56, 21.42, 19.98, 14.02.

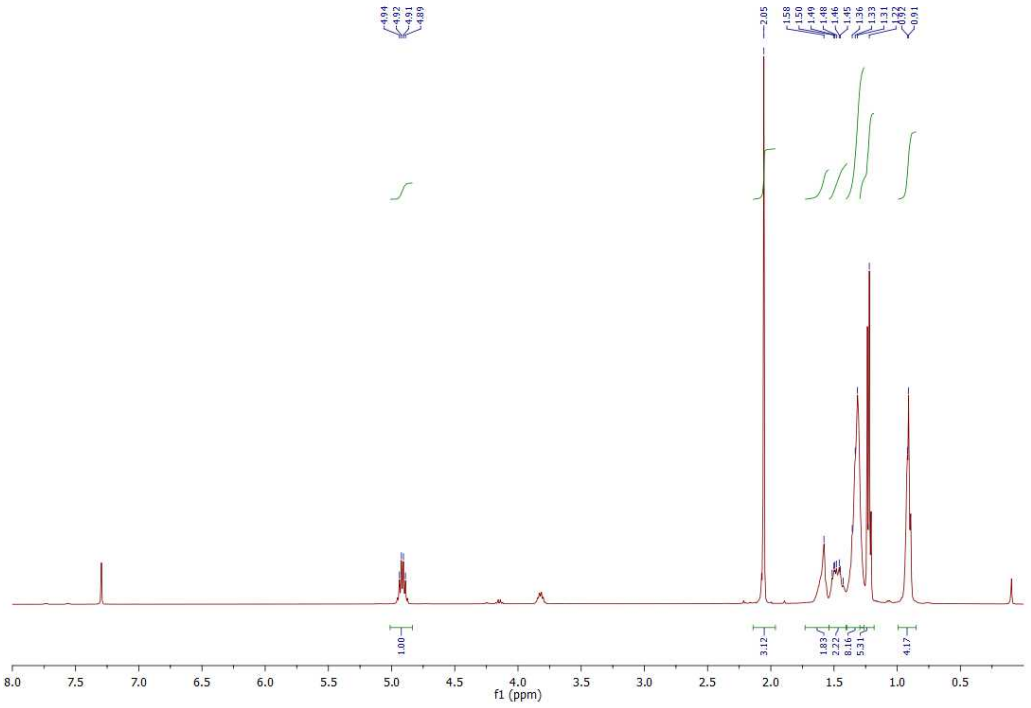

Figure S56: ^{1}H-NMR spectrum (400 MHz, $CDCl_3$) of 2-heptyl acetate

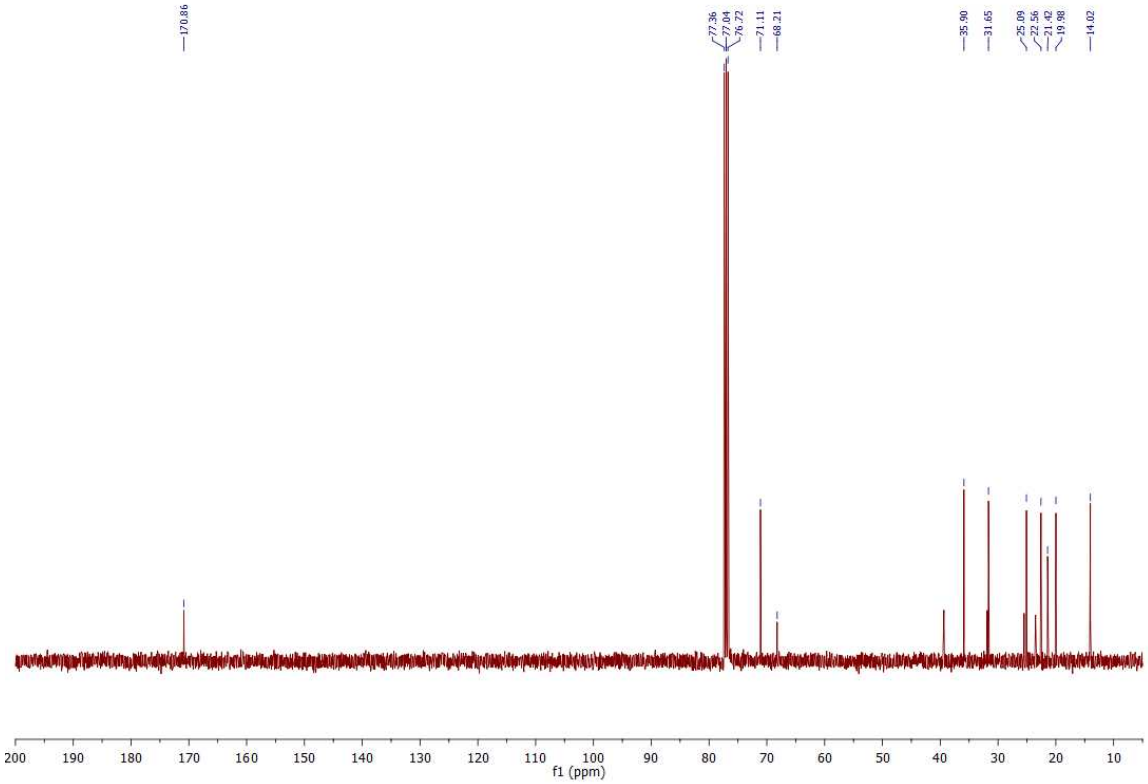

Figure S57: ^{13}C-NMR spectrum (100 MHz, $CDCl_3$) of 2-heptyl acetate